POLITECNICO
MILANO 1863

SCUOLA DI INGEGNERIA INDUSTRIALE
E DELL'INFORMAZIONE

Data-based control for linear systems with stability guarantees

TESI DI LAUREA MAGISTRALE IN AUTOMATION AND CONTROL ENGINEERING-INGEGNERIA DELL'AUTOMAZIONE

Author: **Onur OKCU**

Student ID:	941063 - 10698228
Advisor:	Prof. Marcello FARINA
Co-advisor:	Ing. William D'AMICO
Academic Year:	2021-2022

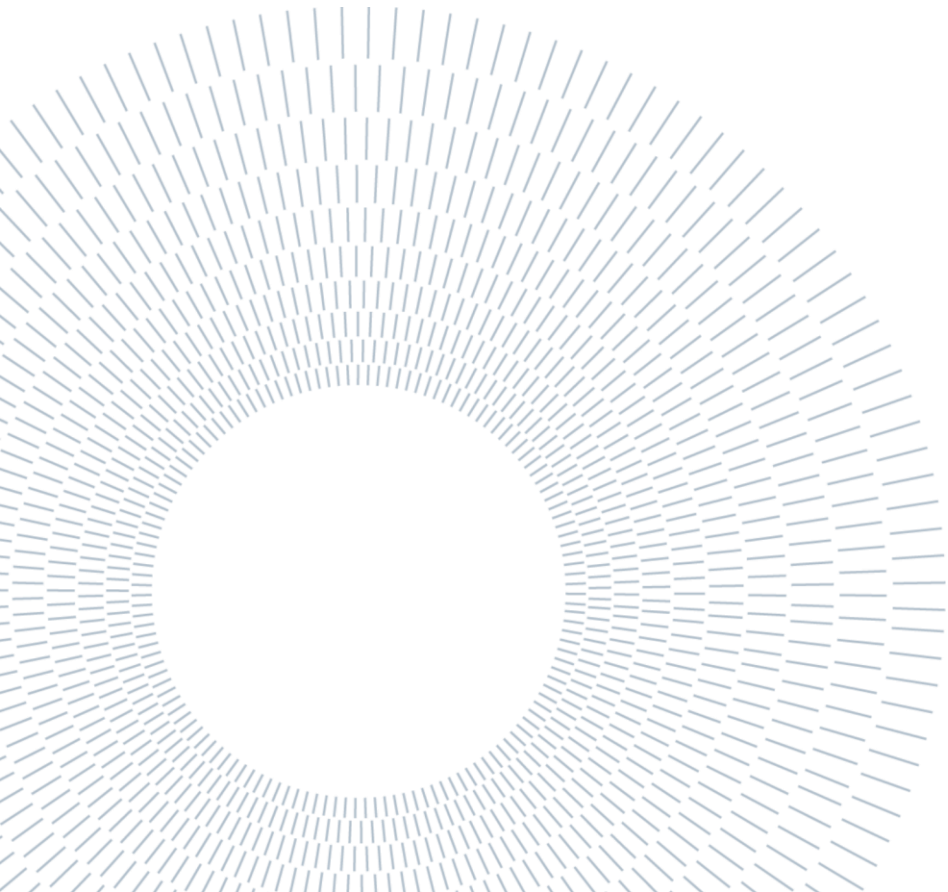

Abstract

The objective of the thesis is to develop a novel data-based control method for linear single-input-single-output (SISO) systems with robust stability guarantees. Given a batch of open-loop data, obtained assuming that the measurement noise is bounded, set membership (SM) identification is performed to obtain an uncertainty set for the system parameters. Based on the previous set, a robust closed-loop stability condition is derived in the form of linear matrix inequalities. The desired performance is enforced through a virtual reference feedback tuning (VRFT) based cost function. The corresponding optimization problem contains only linear matrix inequality (LMI) constraints.

In the first part of the thesis, the theoretical background is provided. In particular, VRFT, direct control design based on controller unfalsification with stability guarantees and SM identification are discussed. Secondly, by combining the SM and VRFT methodologies, a novel data-based control design technique for linear systems with stability guarantees is proposed in different configurations. Lastly, the proposed approach is tested on a simulation example and the results are compared with different state-of-the-art algorithms.

Key-words: Virtual reference feedback tuning; Set Membership identification; data-driven control

Abstract in lingua italiana

L'obiettivo della tesi è quello di sviluppare un metodo di controllo innovativo basato sui dati per sistemi lineari a singolo ingresso e singola uscita (SISO) con garanzie di stabilità robuste. Dato un insieme di dati raccolti in anello aperto, in cui il rumore di misura è limitato, viene eseguita un'identificazione di tipo set membership (SM) per ottenere un insieme di incertezza per i parametri del sistema. Sulla base dell'insieme ottenuto viene derivata una condizione di stabilità robusta per il sistema ad anello chiuso. Le prestazioni desiderate vengono imposte attraverso una funzione di costo basata sulla tecnica del virtual reference feedback tuning (VRFT). Il corrispondente problema di ottimizzazione contiene solo vincoli con disuguaglianze matriciali lineari (LMI).

Nella prima parte della tesi viene fornito il background teorico. In particolare vengono trattati il VRFT, il progetto di controllo diretto con garanzie di stabilità basato sul metodo della non falsificazione del controllore e l'identificazione di tipo SM. In secondo luogo, combinando le metodologie di SM e VRFT, viene proposta una nuova tecnica di progettazione del controllore basata sui dati per sistemi lineari con garanzie di stabilità in tre diverse configurazioni. Infine, l'approccio proposto viene messo alla prova su un esempio di simulazione e i risultati vengono confrontati con quelli ottenuti applicando algoritmi da letteratura.

Parole chiave: Virtual reference feedback tuning; identificazione Set Membership; controllo basato sui dati

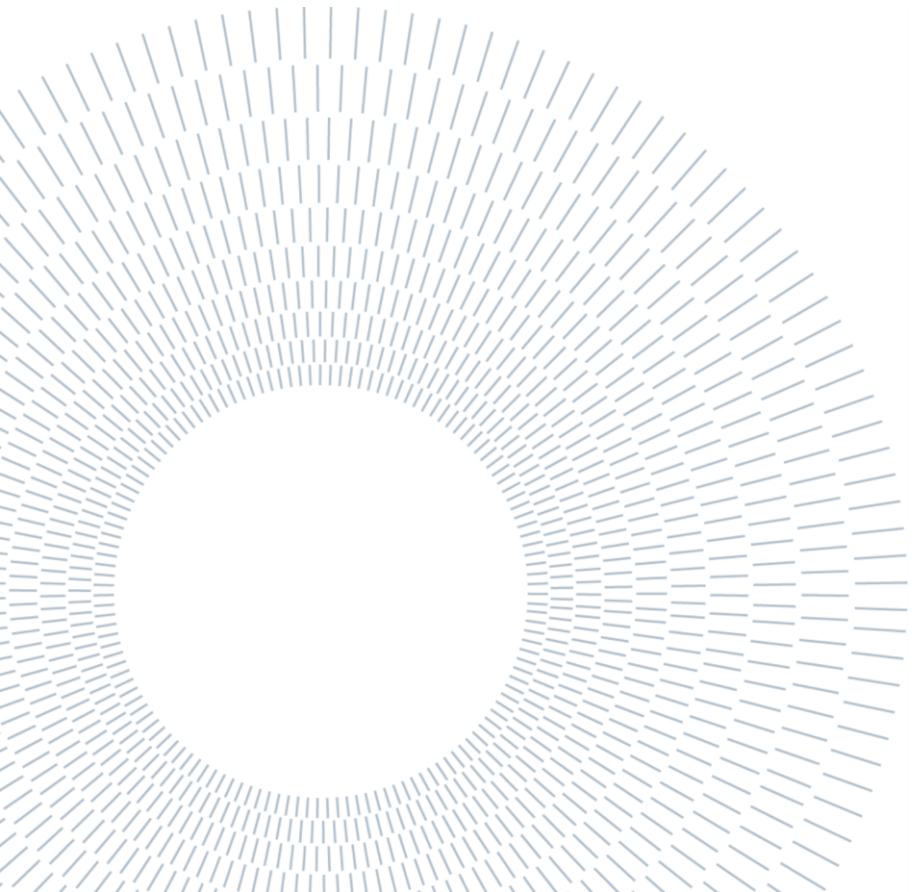

Contents

1. Introduction

1.1 Data-based control design

The design of controllers based on data is of great importance in practical applications because this approach allows to save from time-consuming and costly modelling processes. For this reason, many data-driven control methods have been recently developed.

Data-driven control methods can be classified into two groups: direct methods such as iterative feedback tuning [27], virtual reference feedback tuning [17-21,25], correlation-based tuning [26], and indirect methods which may rely on recurrent neural networks (RNN) [30], Hammerstein-Wiener models [28], AutoRegressive models with eXogenous (ARX) variables for the plant identification phase [29].

Among them, direct methods have a number of advantages, since they allow to prevent problems caused by unmodeled dynamics and overcome model-mismatch problems. Unlike the indirect methods, in direct methods an identification phase of the mathematical model of the plant is not required. Indeed, direct methods directly target the final aim of tuning the controller parameters.

The focus of this thesis is VRFT, i.e., a non-iterative direct data-driven control design approach based on a set of input/output data. Since it is non-iterative, only one batch of experimental data is required for the tuning of the controller. VRFT has been first introduced in case of linear systems [20,21] but has been also extended to nonlinear systems [17,18]. Even if most of the work in the literature regarding VRFT focuses on SISO systems, some recent contributions are available for MIMO systems as well [19].

Even though VRFT is advantageous for several reasons, the resulting closed-loop system is not guaranteed to be stable. In the data-driven framework, in order to verify whether the controller guarantees the closed-loop stability or not, some approaches have been developed for the data-driven controller certification problem such as using ν-gap metric [23], using closed-loop data for the estimation of H_∞-norm based on Markov parameters [22] or taking advantage of the unfalsified control theory in order to verify the controller iteratively [24].

Among them, the latter approach is proposed in [1] for the tuning of an optimal direct data-driven controller with stability guarantees. However, the algorithm results in conservative solutions due to small gain arguments. In addition, the stability condition is not enforced directly in the controller tuning phase but is tested a posteriori.

1.2 Contribution of the thesis

In this thesis, we propose an alternative approach which provides the desired closed-loop behavior as well as the closed-loop stability guarantees. In order to achieve this goal, set membership (SM) identification is used. SM method provides a set of candidate models based on a set of input/output data and these models are used to confer robust stability conditions in a VRFT-based linear matrix inequality-based optimization problem.

1.3 Structure of the thesis

The thesis is organized as follows:

Chapter 2 introduces all the theoretical background. In particular VRFT, direct control design based on controller unfalsification with stability guarantees, and set membership identification are discussed.

Chapter 3 introduces the proposed approach, i.e., the data-based control for linear systems with stability guarantees and three alternative possible control schemes are investigated.

Chapter 4 is devoted to testing the proposed approach on an example consisting of three cascaded tanks. The simulation results are given and compared with the ones obtained with the direct control design based on controller unfalsification with stability guarantees.

Chapter 5 provides conclusions and future developments for the thesis.

2. Theoretical background

2.1 Virtual reference feedback tuning

In this section we describe the VRFT algorithm proposed in [5], used to design data-based controllers for discrete-time systems.

2.1.1 Problem formulation

In this section we introduce the problem addressed in [5].

We consider the following system

$$y(t) = P(d)u(t) + n(t) \tag{2.1}$$

where $y(t)$ is the plant output corrupted by the noise $n(t)$, $u(t)$ is the input of the system, $P(d)$ is the unknown plant transfer function of the system and d is the unit backward shift operator. Throughout this section, for the sake of simplicity, we neglect the effect of noise, i.e., $n(t) = 0$. However, the algorithm in [5] can be extended to account for the effect of the noise.

The discrete-time linear time-invariant (LTI) plant can be described by the following transfer function

$$P(d) = \frac{n_0 + n_1 d + \cdots + n_{n_n} d^{n_n}}{1 + m_1 d + \cdots + m_{n_m} d^{n_m}} \tag{2.2}$$

We will consider systems with one time step delay between the input and the output as stated in Assumption 2.1.

Assumption 2.1.

The input-output delay of the system is equal to 1.

Since VRFT is a non-iterative direct approach, only one dataset $\mathcal{D}$ of input-output pairs is required and $\mathcal{D}$ is obtained from an open-loop experiment.

$$\mathcal{D} = \{u(t), y(t) : t = 0, \dots, N\} \tag{2.3}$$

The problem addressed in this chapter consists of developing a suitable controller conferring to the system performances as similar as possible to the ones of a reference model directly from data. The reference model is selected by the user based on the desired closed-loop performance. The controller is denoted $C(d, \theta)$ and the problem consists of tuning the controller parameter vector θ by means of the available data set $\mathcal{D}$.

2.1.2 Control scheme and controller family

In this section we introduce the proposed control scheme and present the possible controller families.

The proposed control scheme is represented in Figure 2.1, where $e(t)$ denotes the error signal, $r(t)$ is the reference signal and $C(d, \theta)$ is the controller parametrized by the vector θ.

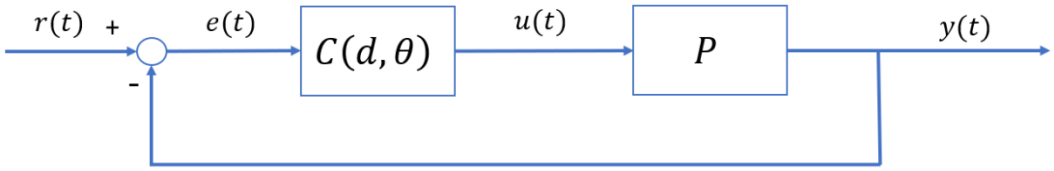

Figure 2.1: The proposed control scheme

The controller family $\mathcal{C}$ consists of candidate controllers that are functions of the design parameter θ. The general structure of the controller family parametrized with θ is the following

$$\mathcal{C} := \{C(d, \theta) = \beta^T(d)\theta\} \tag{2.4}$$

where $\theta = [\theta_1 \quad \theta_2 \quad \dots \quad \theta_n]^T \in \mathbb{R}^n$ is the vector of parameters to be tuned and $\beta(d) = [\beta_1(d) \quad \beta_2(d) \quad \dots \quad \beta_n(d)]^T$ is a set of linear discrete-time transfer functions.

2.1.3 Reference model definition and discrepancy function

In this section we discuss the choice of the reference model. Moreover, we show how to build the discrepancy function between the reference model and the closed-loop system.

The reference model M defines the desired closed-loop performance and provides the ideal linear transfer function from the reference r to the output measurement y.

The typical reference model representation of M is the following

$$M(d) = \frac{b_1 d + \cdots + b_{n_b} d^{n_b}}{1 + a_1 d + \cdots + a_{n_a} d^{n_a}} \tag{2.5}$$

The corresponding time domain representation can be obtained as

$$\begin{aligned} y(t) = -a_1 y(t-1) - \cdots - a_{n_a} y(t-n_a) + b_1 r(t-1) + \cdots \\ + b_{n_b} r(t-n_b) \end{aligned} \tag{2.6}$$

Note that a delay of at least 1 step is required to $M(d)$ consistently with Assumption 2.1.

The control objective is to have a complementary sensitivity function as similar as possible to the reference one. In order to achieve this goal, the classical control scheme in Figure 1.1 is used and the problem becomes the tuning of the controller parameters. To do that, the following discrepancy function must be minimized:

$$\mathcal{J}_{MR}(\theta) := \left\| \left(\frac{P(d)C(d,\theta)}{1 + P(d)C(d,\theta)} - M(d) \right) W(d) \right\|^2 \tag{2.7}$$

where $\|\cdot\|$ is the Euclidian norm and $W(d)$ is a user-defined weighting function. However, we cannot minimize in practice the discrepancy function in (2.7) since the plant transfer function P is not known. The alternative cost function is described in Section 2.1.4.

2.1.4 VRFT cost function

In this section we show how it possible obtain an equivalent cost function to (2.7) which does not require any knowledge on the plant.

The dataset $\mathcal{D}$ in (2.3) is used. We define as $\tilde{u}$ and $\tilde{y}$ the vectors collecting the available input and output data, respectively.

We define the virtual reference signal $\tilde{r}$ as follows

$$\tilde{r} = M^{-1}[\tilde{y}] \tag{2.8}$$

The term "virtual", in this framework, denotes that $\tilde{r}$ is not a real signal like the input and the output. Theoretically, if the virtual reference signal is forced as reference signal to the desired closed-loop system, i.e., M, it produces the u and y pairs. Moreover, if the controller family is rich and the reference signal is exciting enough, this aim may be achievable.

As depicted in Figure 2.2, the virtual error in the closed-loop system is defined as follows

$$\tilde{e} = \tilde{r} - \tilde{y} \tag{2.9}$$

In order to have the virtual error different from 0, Assumption 2.2. must hold.

Assumption 2.2.

$M(d) \neq 1$.

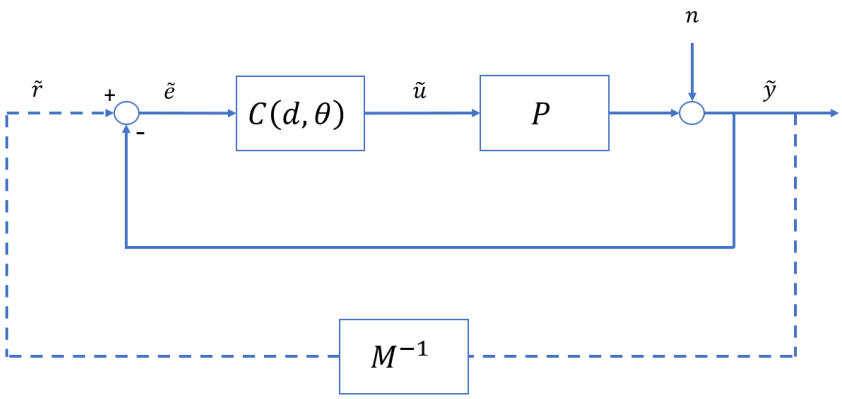

Figure 2.2: The closed loop system and the virtual signals

The objective is to design a control law $C(d,\theta)$ that confers the closest closed-loop behavior with the selected reference model M. An alternative P-free objective function equivalent to (2.7) can be written as follows

$$\mathcal{J}_{VRFT}^{N}(\theta) := \frac{1}{N}\|\tilde{u}_L - C(d,\theta)\tilde{e}_L\|^2 \tag{2.10}$$

where $\tilde{u}_L$ and $\tilde{e}_L$ denote pre-filtered signals with a suitable filter $L(d)$. These signals are defined as follows

$$\tilde{u}_L = L(d)\tilde{u} \tag{2.11a}$$

$$\tilde{e}_L = L(d)\tilde{e} \tag{2.11b}$$

The filter $L(d)$ is required especially when the "ideal controller" does not belong to the chosen controller class. The "ideal controller" can be defined as the controller that leads to perfect matching with M when it is interconnected in the closed-loop system. If the "ideal controller" exists, the minimization of $\mathcal{J}$ and $\mathcal{J}_{VRFT}^N$ coincide and it is possible to find a solution to original problem throughout the minimization of the alternative cost function (2.10). On the other hand, the filter $L(d)$ allows us to find a "nearly minimizer" of $\mathcal{J}$ through $\mathcal{J}_{VRFT}^N$ when the perfect matching cannot be provided. More details regarding the filter design and implementation are in [5].

Finally, enforcing the linear structure of the controller, i.e., $C(d,\theta) = \beta^T(d)\theta$, equation (2.10) can be rewritten as follows

$$\mathcal{J}_{VRFT}^N(\theta) = \frac{1}{N}\sum_{t=1}^{N}(u_L(t) - \varphi_L(t)\theta)^2 \tag{2.12a}$$

$$\varphi_L(t) = \beta(d)e_L(t) \tag{2.12b}$$

Note that the objective function in (2.12a) is a purely data-dependent cost. The corresponding optimal parameter vector θ_N^* for the controller can be directly calculated as follows

$$\theta_N^* = \underset{\theta}{\operatorname{argmin}}\, \mathcal{J}_{VRFT}^N(\theta) = \left[\sum_{t=1}^{N}\varphi_L(t)\varphi_L(t)^T\right]^{-1}\sum_{t=1}^{N}\varphi_L(t)u_L(t) \tag{2.13}$$

2.1.5 The algorithm

The steps of the virtual reference feedback tuning algorithm are the following

1. Collect a dataset $\mathcal{D}$ with an open-loop experiment. Select the reference model M, and the controller family $\mathcal{C}$.
2. Find the virtual reference $\tilde{r}$ and compute the corresponding virtual error $\tilde{e}$.
3. Pre-filter the measured data and obtain $\tilde{u}_L$ and $\tilde{e}_L$ as in equation (2.11).
4. Compute θ_N^*, i.e., the optimal parameter vector of the controller, as in (2.13).

2.2 Direct control design based on controller unfalsification with stability guarantees

In this section we introduce a non-iterative direct data-driven control design method proposed in [1], i.e., the direct control design based on controller unfalsification with stability guarantees.

As stated in [1], one of the main drawbacks of direct methods is the absence of a plant model. As the process to be controlled is not identified, a mechanism to validate/falsify the controller is necessary. This motivates the unfalsification method discussed here. Unlike other stability-oriented approaches, the proposed approach does not require to consider minimum phase plants or the knowledge of possible unstable zeros. Furthermore, even if having a stable plant is an assumption for the application of the algorithm, unstable plants can be also addressed just after a basic stabilization procedure with a simple cascade controller [1].

2.2.1 Problem formulation

In this section we introduce the problem that is formulated and solved in [1]. The proposed approach is an alternative to classic VRFT [17-21] but, in addition, allows to guarantee closed-loop stability thanks to a suitable stability test.

The method in [1] is a non-iterative direct approach. Thus, a single batch of experimental data ($\mathcal{D}$ see equation (2.3)) is required and is directly used for the controller identification.

The following assumption is requested for consistency.

Assumption 2.3.

The input $u(t)$ is a stationary signal independent of the additive output disturbance $n(t)$.

Recall that $P(d)$ is the unknown plant transfer function. Such unknown discrete-time LTI plant can also be expressed as

$$P(d) = \frac{B(d)}{A(d)} \tag{2.14}$$

The terms $A(d)$ and $B(d)$ are unknown polynomials of the form of $A(d) = 1 + a_1 d + \cdots + a_{n_a} d^{n_a}$ and $B(d) = b_0 + b_1 d + \cdots + b_{n_b} d^{n_b}$. For the sake of simplicity, we will consider the assumption that $P(d)$ is stable, as stated in Assumption 2.4. The unstable plant case is discussed in [1].

Assumption 2.4.

The roots of $A(d)$ strictly lie in the unit circle.

The addressed problem consists of providing both closed-loop stability and desired closed-loop performance.

2.2.2 Proposed control scheme and controller family

In this part, we introduce the proposed control scheme for the given problem formulation and the candidate controllers will be restricted to lie in a given controller family.

The proposed control scheme is provided in Figure 2.3. $C(d,\theta)$ is the LTI controller to be tuned and $r(t)$ is the reference signal.

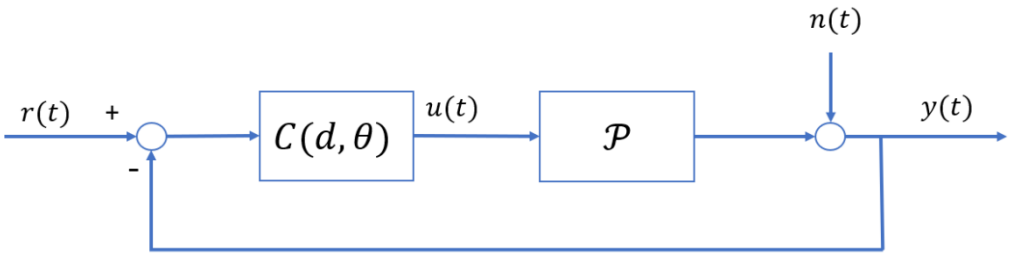

Figure 2.3: The closed loop system configuration

The controller family $\mathcal{C}$ consists of candidate LTI controllers that are function of the design parameter θ, i.e.,

$$\mathcal{C} \coloneqq \{C(d,\theta), \theta \in \Theta \subset \mathbb{R}^{n_\theta}\} \tag{2.15}$$

where Θ is a compact set and n_θ is the number of parameters to be tuned. The candidate LTI controllers $C(d,\theta)$ must have the following transfer function form

$$C(d,\theta) = \frac{S(d,\theta)}{R(d,\theta)} \tag{2.16}$$

As discussed in [1], considering a parametric form of the controller family with some fixed parts (e.g., an integrator) helps to fulfill some tracking/rejection purposes. Therefore, it is possible to express both the denominator and the numerator as follows

$$C(d,\theta) = \frac{\bar{S}(d,\theta)S^*(d)}{\bar{R}(d,\theta)R^*(d)} \tag{2.17}$$

Here, $S^*(d)$ and $R^*(d)$ have possibly unstable roots. They are fixed coprime polynomials and $R^*(0) = 1$. For example, to equip the controller with integral action, $R^*(d) = 1 - d$ is a typical choice.

Moreover, the parameter vector can be constructed with coefficients of $\bar{S}(d,\theta) = s_0 + s_1 d + \cdots + s_{n_s} d^{n_s}$ and $\bar{R}(d,\theta) = 1 + r_1 d + \cdots + r_{n_r} d^{n_r}$. In this way,

$$\theta = [s_0 \quad \cdots \quad s_{n_s} \quad r_1 \quad \cdots \quad r_{n_r}]^T \tag{2.18}$$

2.2.3 Reference model definition and related discrepancy function

In order to have both satisfactory performance and stabilization at the same time, the approach requires to define two reference models: $Q(d)$ and $W(d)$. While $Q(d)$ is the desired input sensitivity function and allows to enforce stability, $W(d)$ is the desired complementary sensitivity function and is responsible for the output performance.

Note that $Q(d)$ and $W(d)$ are a priori selected, consistently with Assumption 2.5.

Assumption 2.5.

a. $W(d)$ is strictly proper.
b. $Q(d)$ and $W(d)$ are stable.

$Q(d)$ and $W(d)$ must be also consistent with the controller family $\mathcal{C}$. Such consistency is an important requirement and will be used to provide a sound robust stability test in the next sections. To guarantee that consistency is fulfilled, Assumption 2.6. is introduced.

Assumption 2.6.

a. All roots of $S^*(d)$ are zeros of $W(d)$
b. All roots of $R^*(d)$ are zeros of $1 - W(d)$
c. For stable and minimum phase $\bar{Q}(d)$, $Q(d)$ can be decomposed as $Q(d) = S^*(d)\bar{Q}(d)$

According to Figure 2.3, the following equations can be obtained

$$u(t) = \frac{C(d,\theta)}{1 + P(d)C(d,\theta)} r(t) - \frac{C(d,\theta)}{1 + P(d)C(d,\theta)} n(t) \tag{2.19a}$$

$$y(t) = \frac{P(d)C(d,\theta)}{1 + P(d)C(d,\theta)} r(t) + \frac{1}{1 + P(d)C(d,\theta)} n(t) \tag{2.19b}$$

Notably, the input sensitivity and complementary sensitivity functions are, respectively

$$Q_\theta(d) = \frac{C(d,\theta)}{1 + P(d)C(d,\theta)} \tag{2.20a}$$

$$W_\theta(d) = \frac{P(d)C(d,\theta)}{1 + P(d)C(d,\theta)} \tag{2.20b}$$

The problem we address can be formulated by expressing the discrepancy between each reference model and related sensitivity function, separately

$$J(\theta) = D(Q_\theta(d), Q(d)) \tag{2.21a}$$

$$V(\theta) = D(W_\theta(d), W(d)) \tag{2.21b}$$

where $D(a,b)$ is a distance measure between a and b.

While the minimization of $V(\theta)$ is standard in VRFT or similar approaches and induces the desired closed-loop behavior, the minimization of $J(\theta)$ is used to foster the closed-loop system stability, as discussed in [1]. In fact, consider the "ideal" controller, i.e., the one makes $Q_\theta(d) = Q(d)$, denoted $C_Q(d)$.

We compute that

$$C_Q(d) = \frac{Q(d)}{1 - Q(d)P(d)} \tag{2.22}$$

In view of Assumption 2.4. (i.e., stability of the plant), $C_Q(d)$ guarantees closed loop stability, as more detailly discussed in [1].

However, having two different reference models makes the design problem multi-objective because, generally, it is not possible to guarantee the minimization of the two discrepancies at the same time. Furthermore, since $P(d)$ is unknown, the minimization of $J(\theta)$ and $V(\theta)$ is achieved by formulating alternative optimization problems, defined in Section 2.2.4.

2.2.4 Optimization problem

Two reference models and the related cost functions have been already introduced in Section 2.2.3. In this section, we discuss how the two discrepancy functions, $J(\theta)$ and $V(\theta)$, are redefined with the available experimental data and independently of the unknown plant transfer function. Finally, it is shown how they are collected in a unique cost function.

In Figure 2.4, the fictitious signals that are obtained through reference models and their real (non-virtual) signal counterparts are shown.

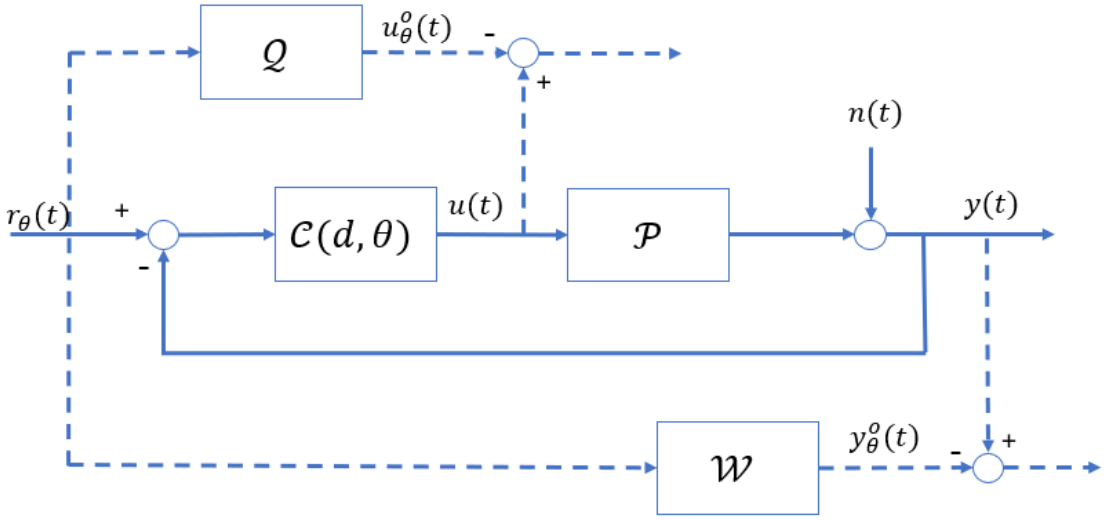

Figure 2.4: The closed-loop system and reference models

Considering Figure 2.4, the fictitious reference is defined as follows

$$r_\theta(t) = C(d,\theta)^{-1}u(t) + y(t), t = 0, \dots, N \tag{2.23}$$

Consistently, the fictitious input and output can be obtained as follows

$$u_\theta^o(t) \coloneqq Q(d)r_\theta(t) \tag{2.24a}$$

$$y_\theta^o(t) \coloneqq W(d)r_\theta(t) \tag{2.24b}$$

$J(\theta)$ and $V(\theta)$ can be minimized by minimizing the following cost functions

$$\mathcal{J}_N(\theta) \coloneqq \|(u - u_\theta^o)|^N\|^2 \tag{2.25a}$$

$$\mathcal{V}_N(\theta) \coloneqq \|(y - y_\theta^o)|^N\|^2 \tag{2.25b}$$

respectively, where $\|x|^N\|^2 \coloneqq \sum_{t=0}^{N} x(t)^2$. Note that:

$$y(t) - y_\theta^o(t) = [1 - W(d)]P(d)u(t) - C^{-1}(d,\theta)W(d)u(t) + [1 - W(d)]n(t) \quad (2.26a)$$

$$u(t) - u_\theta^o(t) = u(t) - Q(d)P(d)u(t) - C^{-1}(d,\theta)Q(d)u(t) - Q(d)n(t) \quad (2.26b)$$

Under Assumption 2.3. and also considering that the disturbance term $n(t)$ does not depend on θ, it can be concluded that, as N goes to infinity, the solution tends to be independent of $n(t)$.

In a multi-objective optimization problem of this type, where the two optimization objectives are possibly conflicting, the Pareto optimal solution is achieved by minimizing a cost function defined as a linear combination of the individual ones in (2.25a) and (2.25b). Namely, the selected cost is

$$(1 - \delta)\, \mathcal{J}_N(\theta) + \delta \mathcal{V}_N(\theta) \quad (2.27)$$

where $\delta \in [0,1]$ which can be used to trade the optimality (i.e., obtained with $\delta = 1$) and the stability (i.e., with $\delta = 0$).

Before defining the optimal solution vector, we need to restrict the parameter vector in a suitable set Θ_S. Θ_S is defined as a subset of Θ in which $C^{-1}(d,\theta)Q(d)$ is stable. The definition of such subset is needed because, whenever the stability of $C^{-1}(d,\theta)Q(d)$ is provided, the errors defined in equation (2.27) are numerically stable thanks to Assumption 2.6. The proof is shown in [1].

To conclude, the optimal parameter vector $\theta_N^*(\delta) = [{s_0}^* \quad \dots \quad {s_{n_s}}^* \quad {r_1}^* \quad \dots \quad {r_{n_r}}^*]^T$ is defined as a function of δ as follows

$$\theta_N^*(\delta) = \underset{\theta \in \Theta_S}{\operatorname{argmin}} \{(1 - \delta)\, \mathcal{J}_N(\theta) + \delta \mathcal{V}_N(\theta)\} \quad (2.28)$$

2.2.5 Stability test via controller unfalsification

In this section, we describe the test implemented to verify the stability of the closed-loop system.

According to [31], the term "unfalsification" is used to denote an approach that allows to discard iteratively controllers that do not satisfy certain requirements. In our case such requirement is closed-loop stability.

Ideally, when we set $\delta = 0$, then we can obtain, as a solution to (2.28), $C(d, \theta^*) = C_Q(d)$. This, as discussed in Section 2.2.3, guarantees the closed-loop stability. However, when $C_Q(d)$ cannot be fully achievable (for example when it does not lie in the controller family) or we also need to improve the performance through desired complementary sensitivity objective function $\mathcal{V}_N(\theta)$, a tool for stability test is essential.

First, we start with studying the relation between closed-loop stability and input discrepancy $u - u_\theta^o$. The input discrepancy could be rewritten as follows

$$u(t) - u_\theta^o(t) = \Delta_Q(\theta, d)Q(d)u(t) - Q(d)n(t) \tag{2.29}$$

where

$$\Delta_Q(d, \theta) = {C_Q}^{-1}(d) - C^{-1}(d, \theta) \tag{2.30}$$

Thanks to standard small gain arguments the following theorem could be proven.

Theorem 2.1.

Let $\theta \in \Theta_S$, then if

$$\left\| Q(d)\Delta_Q(d, \theta) \right\|_\infty < 1 \tag{2.31}$$

then the controller $C(d, \theta)$ internally stabilizes the unknown plant P.

Thanks to the Theorem 2.1., we have finally a tool for closed-loop stability check. The H_∞ norm in (2.31) can be computed as follows

$$\left\| Q(d)\Delta_Q(d, \theta) \right\|_\infty = \sup_{\omega \in [-\pi, \pi]} \frac{|\hat{u}(\omega) - \hat{u}_\theta^o(\omega)|}{|\hat{u}(\omega)|} \tag{2.32}$$

where $\hat{u}(\omega)$ and $\hat{u}_\theta^o(\omega)$ are the discrete Fourier transforms of $u(t)$ and $u_\theta^o(t)$, respectively. The given relation is valid only when $|\hat{u}(\omega)| > 0$ for all frequencies in the range and only in case of infinite-length data set.

In practice, after obtaining the input discrepancy $u - u_\theta^o$ with the help of the data set on hand, standard non-parametric identification techniques such as windowed Empirical Transfer Function Estimation (ETFE) can be implemented to have an estimation on $\left\|Q(d)\Delta_Q(\theta, d)\right\|_\infty$ for any parameter vector θ.

On the other hand, the finite data set length and ignoring the effect of the disturbance term $n(t)$ require to introduce scalar $\tilde{\alpha}$ which creates more reliability to the inequality, the inequality becomes as follows

$$\left\|Q(d)\Delta_Q(d, \theta)\right\|_\infty < 1 - \tilde{\alpha} \tag{2.33}$$

2.2.6 Tuning procedure and algorithm

In this section the algorithm is presented step-by-step. Then, the results of the algorithm are discussed and the comparison with VRFT are shortly given.

The steps to be followed for tuning the data-driven controller with stability test are listed below.

1. Provide the data set $\mathcal{D}$ with open-loop experimental input-output pairs, the input and complementary sensitivity reference models $Q(d)$ and $W(d)$, the controller family $\mathcal{C}$ and the scalar $\tilde{\alpha}$ used in Section 2.2.5
2. Set $\delta = 0$. Solve (2.28) and obtain $\theta_N^*(0)$. Estimate $\left\|Q(d)\Delta_Q(d, \theta_N^*(0))\right\|_\infty$
3. While $\left\|Q(d)\Delta_Q(d, \theta_N^*(0))\right\|_\infty < 1 - \tilde{\alpha}$ and $\delta \leq 1$
    - Increase δ (i.e., set $\delta = \delta + \Delta\delta$)
    - Solve (2.28) and obtain $\theta_N^*(\delta)$
    - Estimate $\left\|Q(d)\Delta_Q(d, \theta_N^*(0))\right\|_\infty$
4. Set $\delta^* = \delta$, i.e., the larger value of δ such that the stability can be verified

Notice that, in case $\left\|Q(d)\Delta_Q(d, \theta_N^*(0))\right\|_\infty \geq 1$, the controller family results unsuitable, or the data are not informative enough. Such problem can be handled by re-running the algorithm with a new extended controller family or re-performing an open-loop experiment more informative about the process dynamics.

It is important to emphasize that even in case $\delta = 1$, i.e., when only the output performance is considered, the proposed approach differs from the classic VRFT. In fact, in the unfalsified control framework, the fictitious reference is retrieved from the candidate controller term inversion $C^{-1}(d, \theta)$. On the other hand, in VRFT the virtual reference is obtained by the reference model inversion $W^{-1}(d)$.

2.3 Set membership identification

According to [11], set membership (SM) methods have been largely investigated in the last 25 years. The SM approach, in general, can be used to estimate any generic function of a problem element with error-corrupted available data.

SM methods rely upon the assumption of unknown but bounded (UBB) error. This is due to the fact that the more classical random additive noise assumption is not practical for some cases. On the other hand, the UBB error description is more realistic and less demanding compared to statistical error description.

Set membership identification has been first introduced in case of linear systems [14-16] but has been also extended to nonlinear systems [5,10,11] and piecewise affine models [4]. Some recent contributions use SM approaches to derive prediction and simulation models with guaranteed accuracy, e.g., [8,12]. Interestingly, SM is a framework that can be widely combined with control design methodologies such as adaptive model predictive control [9] and model predictive control [7].

In this work, set membership is used in view of the fact that, instead of identifying a unique model, it provides a set of candidate models based on a finite set data corrupted by UBB measurement noise. These models will be used in this thesis for providing robust stability guarantees for the real system and will be combined with VRFT to enforce desired dynamic performances to the control system.

2.3.1 Problem formulation

In this section we describe how SM identification can be used (see also [2] for details) to identify a set of models compatible with the UBB noise-corrupted available data.

The linear time-invariant system $P(d)$ of order n is assumed to generate the available data. It can be described by the following autoregressive exogenous (ARX) structure:

$$\mathcal{S}: \begin{cases} z(k) = \theta^{o^T} \varphi(k) & \text{(2.34a)} \\ y(k) = z(k) + d(k) & \text{(2.34b)} \end{cases}$$

where $z(k) \in \mathbb{R}$ is the output, $y(k)$ is the output measure, $d(k)$ is a bounded additive measurement noise, $\theta^0 \in \mathbb{R}^{n_a+n_b}$ is the system's parameter and $\varphi(k) \in \mathbb{R}^{n_a+n_b}$ is the regressor defined as:

$$\varphi(k) = \begin{bmatrix} z(k-1) \\ \dots \\ z(k-n_a) \\ u(k-1) \\ \dots \\ u(k-n_b) \end{bmatrix} \tag{2.35}$$

In Figure 2.5, the scheme of the system is provided.

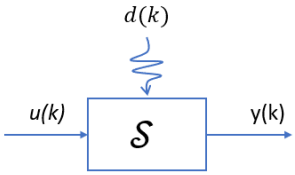

Figure 2.5: System scheme

The goal of Set Membership Identification is to define the set of unknown parameters $\hat{\theta}$ of the predictor.

$$\hat{\mathcal{S}} : \hat{z}(k) = \hat{\theta}^T \hat{\varphi}(k) \tag{2.36}$$

that are compliant with the available data, generated according to (2.34). Variable $\hat{z}(k)$ denotes the one-step ahead predicted output, $\hat{\theta}^\circ \in \mathbb{R}^{n_a+n_b}$ is the set of identified parameters and $\hat{\varphi}(k)$ is the model regressor that includes past available data, i.e.,

$$\hat{\varphi}(k) = \begin{bmatrix} y(k-1) \\ \dots \\ y(k-n_a) \\ u(k-1) \\ \dots \\ u(k-n_b) \end{bmatrix} \tag{2.37}$$

The assumptions stated below are commonly requested for consistent set membership identification.

Assumption 2.7.

a. *The system* $\mathcal{S}$ *is asymptotically stable*
b. $u(k) \in \mathbb{U} \subset \mathbb{R}, \forall k \in \mathbb{Z}$, *where* $\mathbb{U}$ *is compact*
c. $|d(k)| < \bar{d}\,, \forall k \in \mathbb{Z}$, *where* $\bar{d} > 0$ *is known*

2.3.2 Dataset

Some preliminary definitions are required before to dive into the details on the SM method. The set of all possible regressor vectors is defined as ϕ, i.e.,

$$\hat{\varphi}(k) \in \phi \subset \mathbb{R}^{n_a+n_b}, \forall k \in Z \tag{2.38}$$

Set ϕ contains all possible regressor values. In view of Assumption 2.7.b (i.e., that $u(k) \in \mathbb{U}$ for all $k \geq 0$) and Assumption 2.7.a (i.e., regarding the asymptotic stability of the system), such set is compact. Additionally, for any regressor value $\hat{\varphi}(k)$, bearing in mind all possible noise realizations, there exists another compact set, denoted with $y\big(\hat{\varphi}(k)\big)$ that contains all possible 1-step ahead output measurements.

$$\hat{\varphi}(k) \in \phi \Rightarrow y\big(\hat{\varphi}(k)\big) \subset \mathbb{R} \tag{2.39}$$

We are now in the position to define the following set

$$\mathcal{J} := \left\{ \begin{bmatrix} \hat{\varphi} \\ y \end{bmatrix} : y \in y(\hat{\varphi}) \; \forall \hat{\varphi} \in \phi \right\} \subset \mathbb{R}^{n_a+n_b+1} \tag{2.40}$$

The set $\mathcal{J}$ cannot be finitely determined. For this reason, we now define its empirical counterpart $\tilde{\mathcal{J}}^N$, computed based on N available pairs $(y(k), \hat{\varphi}(k))$. More specifically given the N output measures $y(k)$ and regressor values $\hat{\varphi}(k)$, we define:

$$\tilde{\mathcal{J}}^N := \left\{ \begin{bmatrix} \hat{\varphi}(k) \\ y(k) \end{bmatrix}, \quad k = 1, \dots, N \right\} \subset \mathbb{R}^{n_a+n_b+1} \tag{2.41}$$

The following assumption [2] will be required.

Assumption 2.8.

$\forall \beta > 0, \; \exists N < \infty \; such \; that \; d_2(\mathcal{J}, \mathcal{J}^N) \leq \beta$ where $d_2(\mathcal{J}, \mathcal{J}^N)$ is Hausdorff distance between sets $\mathcal{J}$ and $\mathcal{J}^N$.

Assumption 2.8. implies that, if more points are added to the dataset, $\tilde{\mathcal{J}}^N$ will increasingly approximate $\mathcal{J}$. This implies that the results considering the set $\mathcal{J}$ can be generalized also in case its empirical counterpart is considered.

2.3.3 Optimal parameter set and optimal error bound

Considering a given value of $\hat{\theta}$ as a parameter of $\hat{S}$, the error between the true output and predicted one is:

$$\varepsilon\left(\hat{\theta},\hat{\varphi}(k)\right) = z(k) - \hat{z}(k) = z(k) - \hat{\theta}^T\hat{\varphi}(k) \tag{2.42}$$

where $\varepsilon\left(\hat{\theta},\hat{\varphi}(k)\right)$ accounts for both the output noise and fact that $\hat{\theta}$ is in general differs from the ideal parameter vector θ^o. In view of this, we can write the following

$$y(k) = z(k) + d(k) = \hat{\theta}^T\hat{\varphi}(k) + d(k) + \varepsilon\left(\hat{\theta},\hat{\varphi}(k)\right) \tag{2.43}$$

In the light of Assumption 2.7.c, equation (2.43) implies that

$$\left|y(k) - \hat{\theta}^T\hat{\varphi}(k)\right| \leq \bar{d} + \left|\varepsilon\left(\hat{\theta},\hat{\varphi}(k)\right)\right| \tag{2.44}$$

The term $\left|\varepsilon(\hat{\theta},\hat{\varphi}(k))\right|$ can be replaced with $\bar{\varepsilon}(\hat{\theta})$, i.e., the global error bound with respect to all possible regressors and all feasible noise sequences. Such global error bound is defined ideally as

$$\bar{\varepsilon}(\hat{\theta}) = \min_{\varepsilon\in\mathbb{R}} \varepsilon \qquad s.t. \left|y - \hat{\theta}^T\hat{\varphi}\right| \leq \bar{d} + \varepsilon \quad \forall \begin{bmatrix}\hat{\varphi}\\ y\end{bmatrix} \in \mathcal{J} \tag{2.45}$$

The optimal parameter set $\overline{\Theta}$ is defined as the set of all parameters $\hat{\theta}$ that minimize such global error bound. Assume, as a technical assumption, that we can define a compact possibly very large set Ω where $\overline{\Theta}$ surely lies, i.e., $\hat{\theta} \in \Omega$. Thanks to this, we define a set $\overline{\Theta}$ as follows:

$$\overline{\Theta} = \left\{\hat{\theta}: \hat{\theta} = \operatorname*{argmin}_{\theta\in\Omega} \bar{\varepsilon}(\theta)\right\} \tag{2.46}$$

In view of this definition, we can define the optimum global error bound $\bar{\varepsilon}^*$ as follows:

$$\bar{\varepsilon}^* = \bar{\varepsilon}(\overline{\Theta}) = \min_{\theta\in\Omega} \bar{\varepsilon}(\theta) \tag{2.47}$$

Alternatively, the set $\overline{\Theta}$ can be defined as

$$\overline{\Theta} = \left\{\hat{\theta} \in \Omega : \left|y - \hat{\theta}^T\hat{\varphi}\right| \leq \bar{d} + \bar{\varepsilon}^* \quad \forall \begin{bmatrix}\hat{\varphi}\\ y\end{bmatrix} \in \mathcal{J}\right\} \tag{2.48}$$

2.3.4 Estimation of the global error bound

Since set $\mathcal{J}$ is not finitely determined, it is not possible to apply the definitions provided in Section 2.3.3 and compute the optimal parameter set $\overline{\Theta}$ and the global error

bound $\bar{\varepsilon}^*$. For this reason, we compute experimentally $\underline{\lambda} \simeq \bar{\varepsilon}^*$ by solving the following linear program (LP):

$$\underline{\lambda} = \min_{\theta \in \Omega, \lambda \in R^+} \lambda \qquad s.t. \quad \left|y - \hat{\theta}^T \hat{\varphi}\right| \leq \bar{d} + \lambda \quad \forall \begin{bmatrix} \hat{\varphi} \\ y \end{bmatrix} \in \tilde{J}^N \tag{2.49}$$

where $\tilde{J}^N$ is defined as in equation (2.41).

To estimate an optimal error bound, recall that:

$$|y - \theta^T \hat{\varphi}| \leq \bar{d} + \lambda \tag{2.50}$$

is equivalent to impose at the same time

$$y - \theta^T \hat{\varphi} \leq \bar{d} + \lambda \quad \wedge \quad \theta^T \hat{\varphi} - y \leq \bar{d} + \lambda \tag{2.51}$$

i.e.,

$$\left(\theta^T(-\hat{\varphi})\right) - \lambda \leq \bar{d} - y \quad \wedge \quad \theta^T \hat{\varphi} - \lambda \leq \bar{d} + y \tag{2.52}$$

Considering that the previous inequality is defined for all $\begin{bmatrix} \hat{\varphi} \\ y \end{bmatrix} \in \tilde{J}^N$, (2.50) can be written in a compact way as

$$\bar{A}\theta_\lambda \leq \bar{b} \tag{2.53}$$

where

$$\bar{A} = \begin{bmatrix} \varphi(1)^T & -1 \\ \vdots & \vdots \\ \varphi(N)^T & -1 \\ -\varphi(1)^T & -1 \\ \vdots & \vdots \\ -\varphi(N)^T & -1 \end{bmatrix}, \theta_\lambda = \begin{bmatrix} \theta \\ \lambda \end{bmatrix}, \bar{b} = \begin{bmatrix} y(1) + \bar{d} \\ \vdots \\ y(N) + \bar{d} \\ -y(1) + \bar{d} \\ \vdots \\ -y(N) + \bar{d} \end{bmatrix} \tag{2.54}$$

In view of this, the following optimization problem must be solved to compute $\underline{\lambda}$:

$$\underline{\lambda} = \min \lambda \qquad s.t. \quad \bar{A}\theta_\lambda \leq \bar{b} \tag{2.55}$$

Under Assumptions 2.7. and 2.8., the following theorem can be stated [2]:

Theorem 2.2.

1. $\underline{\lambda} \leq \bar{\varepsilon}^*$

2. $\forall \rho \in (0, \bar{\varepsilon}^*] \; \exists N < \infty : \; \underline{\lambda} \geq \bar{\varepsilon}^* - \rho$

Thanks to Theorem 2.2., we can conclude that, under suitable persistence of excitation conditions, $\underline{\lambda} \to \bar{\varepsilon}^*$ as the number of data points increases. A practical way to estimate $\bar{\varepsilon}^*$ from $\underline{\lambda}$ consists of inflating $\underline{\lambda}$ with a multiplying factor α, i.e.,

$$\hat{\bar{\varepsilon}} = \alpha \underline{\lambda}, \;\; \alpha > 1 \tag{2.56}$$

With a sufficiently large dataset and sufficiently exciting signals, it is expected that $\alpha \approx 1$.

2.3.5 Feasible parameter set

After obtaining an estimate $\hat{\bar{\varepsilon}}$ of the global error bound $\bar{\varepsilon}^*$, the next step consists of computing Feasible Parameter Set (FPS). The FPS $\widetilde{\Theta}$ is constructed to contain all the parameter values consistent with the prior knowledge on the system and with the available data. One way to define the FPS is the following

$$\widetilde{\Theta} = \left\{ \hat{\theta} \in \Omega : \; \left| y - \hat{\theta}^T \hat{\varphi} \right| \leq \bar{d} + \hat{\bar{\varepsilon}} \quad \forall \begin{bmatrix} \hat{\varphi} \\ y \end{bmatrix} \in \tilde{J}^N \right\} \tag{2.57}$$

Applying similar argument as the ones used in the Section 2.3.3

$$|y - \theta^T \hat{\varphi}| \leq \bar{d} + \hat{\bar{\varepsilon}} \tag{2.58}$$

The FPS can be defined as the set of parameter values θ fulfilling the inequality

$$A^* \theta \leq b^* \tag{2.59}$$

where

$$A^* = \begin{bmatrix} \hat{\varphi}(1)^T \\ \dots \\ \hat{\varphi}(N)^T \\ -\hat{\varphi}(1)^T \\ \dots \\ -\hat{\varphi}(1)^T \end{bmatrix}, b^* = \begin{bmatrix} y(1) + \bar{d} + \hat{\bar{\varepsilon}} \\ \dots \\ y(N) + \bar{d} + \hat{\bar{\varepsilon}} \\ -y(N) + \bar{d} + \hat{\bar{\varepsilon}} \\ \dots \\ -y(N) + \bar{d} + \hat{\bar{\varepsilon}} \end{bmatrix} \tag{2.60}$$

3. The proposed approach

In this chapter we propose an approach for data-driven control design of unknown linear systems with robust closed-loop stability guarantees. The proposed approach is a data-based control design method. As a prerequisite, a batch of open-loop experimental data, corrupted by unknown but bounded (UBB) measurement noise is assumed to be available. The controller is obtained by minimizing a cost function that penalizes the deviation from the desired closed-loop behavior, as done in VRFT. However, the uncertainty of the system model may lead to control system instability. To cope with such problem, in our approach, first set membership identification is performed (using the same batch of data used for VRFT) and a set of system models, compatible with such data, is derived. Then, through suitable linear matrix inequalities, robust stability is enforced to all models in such set.

3.1 Problem statement

A linear time-invariant system with order n is described by the autoregressive exogenous (ARX) structure (2.34), reported below for the sake of completeness.

$$\mathcal{S}: \begin{cases} z(k) = \theta^{o^T} \varphi(k) & \text{(3.1a)} \\ y(k) = z(k) + d(k) & \text{(3.1b)} \end{cases}$$

Variable $z(k) \in \mathbb{R}$ is the system's output, $y(k)$ is the output measure, $d(k)$ is a bounded additive measurement noise, $\theta^o \in \mathbb{R}^{n_a+n_b}$ is the system's parameter and $\varphi(k) \in \mathbb{R}^{n_a+n_b}$ is the regressor defined as in (2.35). Recall that the input variable $u(k)$ is included in the regressor matrix $\varphi(k)$.

The problem we address is the tuning of the controller based on the available experimental dataset. This controller should provide stability guarantees and the desired closed-loop performance when the system's parameters are unknown.

3.2 Feasible state-space models

The main idea is to use set-membership to define a set of state-space models, i.e., of representations of given system $\mathcal{S}$ compatible with the data. Stability for whole set of state-space models will be guaranteed using suitable LMIs.

Based on the results recalled in Section 2.3., system $\mathcal{S}$ can be rewritten in the following form

$$y(k) = \theta^{o^T}\hat{\varphi}(k) + w(k) \tag{3.2}$$

where the regressor matrix has the following form

$$\hat{\varphi}(k) = \begin{bmatrix} y(k-1) \\ \vdots \\ y(k-n_a) \\ u(k-1) \\ \vdots \\ u(k-n_b) \end{bmatrix} \tag{3.3}$$

The term $w(k)$ accounts both for the measurement noise $d(k)$ and for the prediction error $\varepsilon(k)$.

Importantly, under Assumptions 2.7. and 2.8., the real parameter θ^o, although unknown, is such that $\theta^o \in \widetilde{\Theta}$, being $\widetilde{\Theta}$ the Feasible Parameter Set (FPS) defined in Section 2.3.5. Notably, if $\widetilde{\Theta}$ is bounded, it can be represented as the convex hull of N_v vertices θ^i, $i = 1, \dots, N_V$. More specifically, we can write any $\theta^o \in \widetilde{\Theta}$ as follows

$$\theta^o = \sum_{i=1}^{N_V} \lambda_i \theta^i \tag{3.4a}$$

where

$$\sum_{i=1}^{N_V} \lambda_i = 1 \tag{3.4b}$$

Model (3.2) can be rewritten as the following difference equation

$$\begin{aligned} y(k) = {} & \theta_1^o y(k-1) + \theta_2^o y(k-2) + \ \dots \ + \theta_{n_a}^o y(k-n_a) \\ & + \theta_{n_a+1}^o u(k-1) + \theta_{n_a+2}^o u(k-1) \\ & + \theta_{n_a+2}^o u(k-2) + \ \dots \ + \theta_{n_a+n_b}^o u(k-n_b) + w(k) \end{aligned} \tag{3.5}$$

which admits the following state-space realization:

$$\mathcal{S}:\begin{cases} x(k+1) = F^o x(k) + G^o u(k) + G_w w(k) \\ y(k) = Hx(k) \end{cases} \tag{3.6}$$

The state $x(k)$ is defined as

$$x(k) = \begin{bmatrix} y(k) \\ \vdots \\ y(k-n_a+1) \\ u(k-1) \\ \vdots \\ u(k-n_b+1) \end{bmatrix} \tag{3.7}$$

and the system, input and output matrices are

$$F^o = \begin{bmatrix} \theta_1^o & \theta_2^o & \cdots & \theta_{n_a}^0 & \theta_{n_a+2}^o & \theta_{n_a+3}^o & \cdots & \theta_{n_a+n_b}^o \\ 1 & 0 & \cdots & 0 & 0 & 0 & \cdots & 0 \\ 0 & 1 & \cdots & 0 & 0 & 0 & \cdots & 0 \\ \vdots & \vdots & \ddots & \vdots & \vdots & \vdots & \ddots & \vdots \\ 0 & 0 & \cdots & 0 & 1 & 0 & \cdots & 0 \\ 0 & 0 & \cdots & 0 & 0 & 1 & \cdots & 0 \\ \vdots & \vdots & \ddots & \vdots & \vdots & \vdots & \ddots & \vdots \\ 0 & 0 & \cdots & 0 & 0 & 0 & \cdots & 0 \end{bmatrix}_{(n_a+n_b-1)\times(n_a+n_b-1)}$$

$$G^o = \begin{bmatrix} \theta_{n_a+1}^o \\ 0 \\ \dots \\ 0 \\ 1 \\ 0 \\ \dots \\ 0 \end{bmatrix}_{(n_a+n_b-1)\times 1}, \qquad G_w = \begin{bmatrix} 1 \\ 0 \\ \dots \\ 0 \\ 0 \\ 0 \\ \dots \\ 0 \end{bmatrix}_{(n_a+n_b-1)\times 1} \tag{3.8}$$

$$H = [1 \quad 0 \quad \dots \quad 0]_{1\times(n_a+n_b-1)}$$

Recalling that, in view of equation (3.1a), we can write the unknown $\theta^o \in \widetilde{\Theta}$ as $\theta^o = \sum_{i=1}^{N_V} \lambda_i \theta^i$, also the unknown matrices F^o and G^o can be expressed as convex combinations of known matrices F^i,G^i with $i = 1, \dots, N_V$.

More specifically, we can write

$$[F^o \quad G^o] = \sum_{i=1}^{N_V} \lambda_i \, [F^i \quad G^i] \tag{3.9}$$

and where F^i and G^i are defined as follows

$$F^i = \begin{bmatrix} \theta_1^i & \theta_2^i & \cdots & \theta_{n_a}^i & \theta_{n_a+2}^i & \theta_{n_a+3}^i & \cdots & \theta_{n_a+n_b}^i \\ 1 & 0 & \cdots & 0 & 0 & 0 & \cdots & 0 \\ 0 & 1 & \cdots & 0 & 0 & 0 & \cdots & 0 \\ \vdots & \vdots & \ddots & \vdots & \vdots & \vdots & \ddots & \vdots \\ 0 & 0 & \cdots & 0 & 1 & 0 & \cdots & 0 \\ 0 & 0 & \cdots & 0 & 0 & 1 & \cdots & 0 \\ \vdots & \vdots & \ddots & \vdots & \vdots & \vdots & \ddots & \vdots \\ 0 & 0 & \cdots & 0 & 0 & 0 & \cdots & 0 \end{bmatrix}$$

$$G^i = \begin{bmatrix} \theta_{n_a+1}^i \\ 0 \\ \cdots \\ 0 \\ 1 \\ 0 \\ \cdots \\ 0 \end{bmatrix} \tag{3.10}$$

3.3 State-feedback regulator: condition for robust stability

In this section we introduce the conditions required for robust asymptotic stability for a simple state-feedback regulator. We consider a state-feedback controller of type

$$u(k) = Kx(k) \tag{3.11}$$

We study the conditions required to the gain $K \in \mathbb{R}^{1\times(n_a+n_b-1)}$ for the asymptotic stability of the control system to hold for all possible models (F, G) compatible with the data.

The closed-loop system dynamics is

$$x(k+1) = (F^o + G^o K)x(k) + G_w w(k) \tag{3.12}$$

where, as shown in Section 3.2, F^o and G^o are uncertain but, according to SM identification, are convex combinations of matrices F^i,G^i, known for all $i = 1, \dots, N_V$ and defined according to equation (3.9).

According to [3], the Schur stability of $F^o + G^o K$ is guaranteed if (sufficient condition) $\exists P = P^T > 0$ and K such that

$$\left(F^i + G^i K\right) P \left(F^i + G^i K\right)^T - P < 0\,, \qquad \forall i = 1, \dots, N_V \tag{3.13}$$

Setting $L = KP$, the previous condition is equivalent to the existence of $P = P^T > 0$ and L such that

$$F^i P {F^i}^T + F^i L^T {G^i}^T + G^i L {F^i}^T - G^i L P^{-1} L^T {G^i}^T - P < 0 \tag{3.14}$$

In view of the Schur complement, equation (3.14) is equivalent to the following linear matrix inequality (LMI):

$$\begin{bmatrix} P - F^i P {F^i}^T - F^i L^T {G^i}^T - G^i L {F^i}^T & G^i L \\ L^T {G^i}^T & P \end{bmatrix} > 0 \tag{3.15}$$

Therefore, if such P,L exist, then

$$K = L P^{-1} \tag{3.16}$$

is guaranteed to provide asymptotic stability to the closed-loop system for all possible parametrizations of the model compatible with the available data.

3.4 Control schemes for tracking refence signal

In this section, we show the steps necessary to tune a controller for a system with unknown system parameters that, besides guaranteeing closed-loop stability, provides the desired control system performance. We investigate three alternative possible configurations in the following subsections 3.4.1, 3.4.2 and 3.4.3.

The general form of such control system is displayed in Figure 3.1. $\mathcal{S}$ is the LTI system described in Section 3.1, $\mathcal{R}$ is the regulator to be tuned, $x(k)$ is the system state vector, $y(k)$ is the measured output, $d(k)$ is additive measurement noise, $y^o(k)$ is the time varying reference signal and $M(z)$ is the reference model and z is the unit forward shift operator.

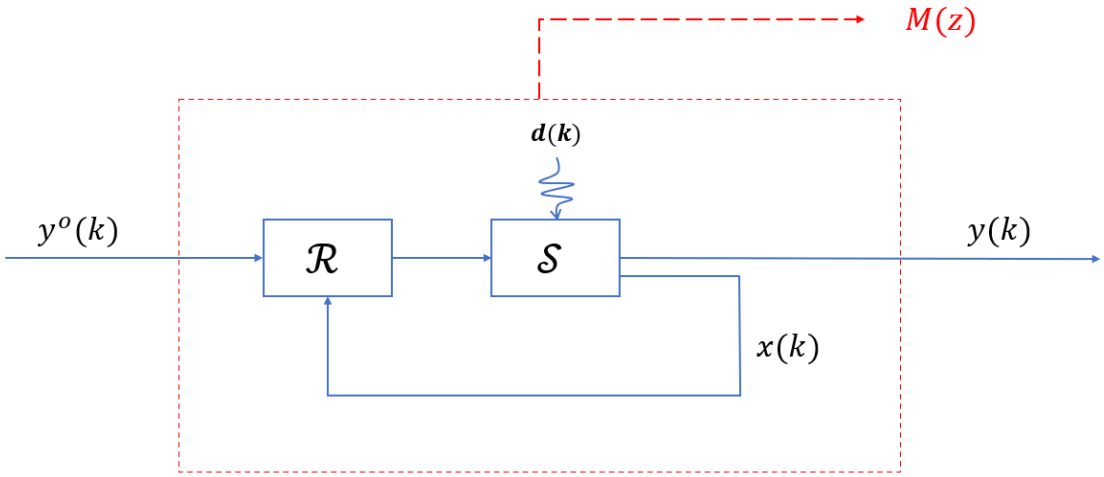

Figure 3.1: General form of tracking scheme

We will combine VRFT and SM to offer both the desired closed-loop performance and closed-loop stability. Such multi-objective problem can be achieved by enforcing stability conditions for all FPS parametrizations, on the main closed-loop performance achievement problem.

3.4.1 Case I: static state-feedback and known system gain

In this part, the regulator with closed-loop stability guarantees and the desired closed-loop performance is derived in the simplified case where the system gain is assumed to be known (or a-priori identified). Consistently, the following assumption is given.

Assumption 3.1.

The system gain μ is known.

Specifically, Assumption 3.1. entails that we know the value of μ such that, in equilibrium conditions, $\bar{z} = \mu\bar{u}$, where $\bar{z}$ and $\bar{u}$ are constant input and output values. We define $\rho = \mu^{-1}$.

3.4.1.1 Proposed control scheme

Considering the general control scheme in Figure 3.1 and a model $\mathcal{S}$ in equation (3.1), we consider the following control law

$$u(k) = \rho y^o(k) + K\big(x(k) - x^o(k)\big) \tag{3.17}$$

where $\rho = \mu^{-1}$ is known (from Assumption 3.1.), $y^o(k)$ is the possibly time-varying reference and $x^o(k)$ can be defined as follows

$$x^o(k) = \begin{bmatrix} y^o(k) \\ \vdots \\ y^o(k) \\ \rho y^o(k) \\ \vdots \\ \rho y^o(k) \end{bmatrix} = \begin{bmatrix} 1 \\ \vdots \\ 1 \\ \rho \\ \vdots \\ \rho \end{bmatrix} y^o(k) = \mu_r^o y^o(k) \tag{3.18}$$

In the construction of $x^o(k)$, the first n_a rows must be equal to $y^o(k)$ and the remaining $n_b - 1$ must be equal to $u^o(k) = \rho y^o(k)$. This is due to the fact that, at steady state, the first states in $x(k)$ correspond to output $y(k)$ and delayed version of it, while the last elements of $x(k)$ correspond to the delayed versions of input $u(k)$, whose desired steady state is $u^o(k) = \rho y^o(k)$.

In Figure 3.2, the configuration obtained when the system gain is known, is shown.

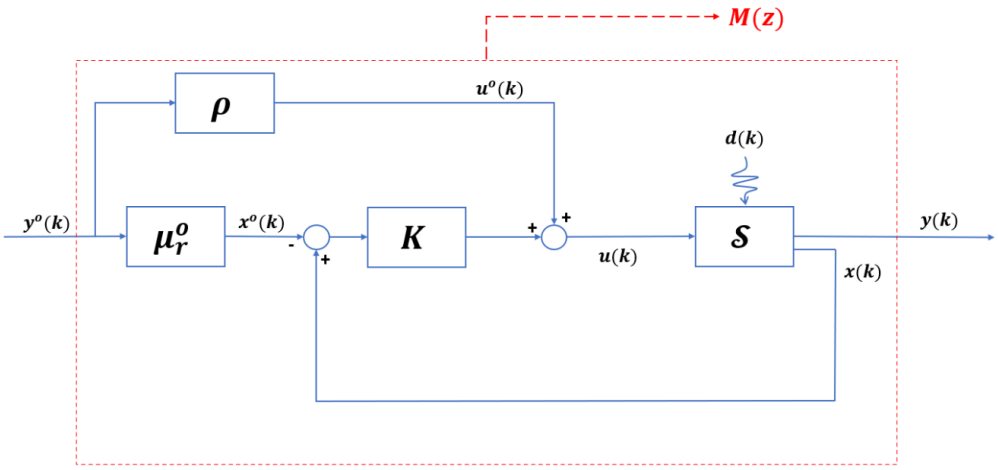

Figure 3.2: Block diagram in case the system gain is known

3.4.1.2 Closed-loop model equations and the stability condition

The control law (3.17) can be rewritten as

$$u(k) = \rho y^o(k) + K\big(x(k) - \mu_r^o y^o(k)\big) \tag{3.19}$$

and can be restated in the following way.

$$u(k) = (\rho - K\mu_r^o) y^o(k) + Kx(k) \tag{3.20}$$

The latter equation allows to redefine the control system, see Figure 3.3.

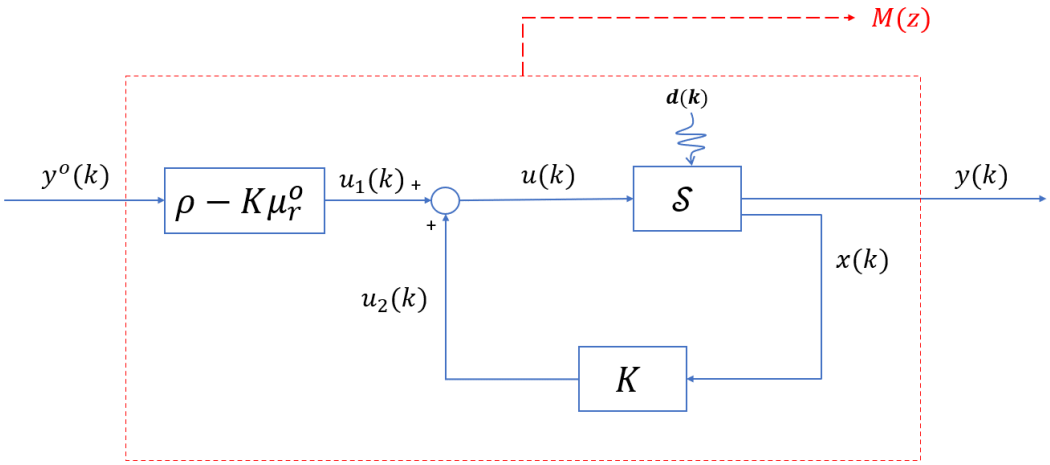

Figure 3.3: Equivalent system scheme when the gain is known

The closed-loop dynamic equation for the state-feedback controller above is

$$x(k+1) = F^{\circ}x(k) + G^{\circ}\big((\rho - K\mu_r^o)y^o(k) + Kx(k)\big) + G_w w(k) \tag{3.21}$$

By means of simple computations, we obtain that

$$x(k+1) = (F^{\circ} + G^{\circ}K)x(k) + G^{\circ}(\rho - K\mu_r^o)y^o(k) + G_w w(k) \tag{3.22}$$

Notice that the closed loop Schur stability is guaranteed if $\exists P = P^T > 0$ and K such that (3.15) holds for all $i = 1, \dots, N_V$.

3.4.1.3 VRFT cost function

As discussed, we assume that an open loop experiment with N-many data points (i.e., experimental data pair $(u(k), y(k))$) is performed. The following VRFT cost function can be defined for any state-feedback controller parameter vector K

$$J_1(K) = \sum_{k=1}^{N-n_r} (u(k) - \rho y^o(k) - (x(k) - \mu_r^o y^o(k))^T K^T)^2 \tag{3.23}$$

where $y^o(k)$ can be derived from $y(k)$: according to system diagram in Figure 3.2, we should enforce

$$y(k) = M(z)y^o(k) \tag{3.24}$$

In view of this, $y^o(k)$ is the *virtual reference*, obtained as

$$y^o(k) = M^{-1}(z)y(k) \tag{3.25}$$

The VRFT cost function can be written in a more compact form as

$$J_1(K) = \left\| \mathbb{u}_1^\circ - \mathbb{x}_1^\circ K^T \right\|^2 \tag{3.26}$$

where

$$\begin{aligned} \mathbb{u}_1^\circ &= \begin{bmatrix} u(1) - \rho y^o(1) \\ \vdots \\ u(N - n_r) - \rho y^o(N - n_r) \end{bmatrix} \\ \mathbb{x}_1^\circ &= \begin{bmatrix} x(1) - \mu_r^o y^o(1) \\ \vdots \\ x(N - n_r) - \mu_r^o y^o(N - n_r) \end{bmatrix} \end{aligned} \tag{3.27}$$

Note that, in the unconstrained case, minimizing (3.26) leads to the following solution,

$$K^T = \mathbb{x}_1^{\circ +} \mathbb{u}_1^\circ \tag{3.28}$$

where $\mathbb{x}_1^{\circ +}$ is the pseudo-inverse of $\mathbb{x}_1^\circ$. At this point, we define the following alternative cost function J_{12} compatible with a reformulation as an LMI optimization problem in variables P and L based on (3.26).

$$J_{12} = \left\| \mathbb{x}_1^{\circ +} \mathbb{u}_1^\circ - K^T \right\|_P^2 \tag{3.29}$$

where

$$K = LP^{-1} \tag{3.30}$$

The cost function J_{12} in equation (3.29) can be rewritten as

$$J_{12} = \mathbb{u}_1^{\circ T} (\mathbb{x}_1^{\circ +})^T P \mathbb{x}_1^{\circ +} \mathbb{u}_1^\circ + LP^{-1}L^T - 2\mathbb{u}_1^{\circ T} (\mathbb{x}^{\circ +})^T L^T \tag{3.31}$$

Note that, minimizing J_{12} is equivalent to minimizing a scalar σ such that

$$\sigma - \mathbb{u}_1^{\circ T} (\mathbb{x}_1^{\circ +})^T P \mathbb{x}_1^{\circ +} \mathbb{u}_1^\circ - LP^{-1}L^T + 2\mathbb{u}_1^{\circ T} (\mathbb{x}^{\circ +})^T L^T \geq 0 \tag{3.32}$$

The latter inequality can be rewritten, thanks to the Schur complement, as

$$\begin{bmatrix} \sigma - \mathbb{u}_1^{\circ T} \left(\mathbb{x}_1^{\circ +}\right)^T P \mathbb{x}_1^{\circ +} \mathbb{u}_1^{\circ} + 2\mathbb{u}_1^{\circ T} (\mathbb{x}^{\circ +})^T L^T & L \\ L^T & P \end{bmatrix} \geq 0 \tag{3.33}$$

3.4.1.4 VRFT-based optimization problem with stability guarantees

Based on the results given in Section 3.4.1.2 and Section 3.4.1.3, we are now in the position to state the main optimization problem that allows to enforce VRFT-like performances and, at the same time, to guarantee robust stability of the closed loop system:

$$\min_{\sigma,P,L} \sigma \tag{3.34a}$$

s.t.

$$\begin{bmatrix} \sigma - \mathbb{u}_1^{\circ T} \left(\mathbb{x}_1^{\circ +}\right)^T P \mathbb{x}_1^{\circ +} \mathbb{u}_1^{\circ} + 2\mathbb{u}_1^{\circ T} (\mathbb{x}^{\circ +})^T L^T & L \\ L^T & P \end{bmatrix} \geq 0 \tag{3.34b}$$

$$\begin{bmatrix} P - F^i P F^{i^T} - F^i L^T G^{i^T} - G^i L F^{i^T} & G^i L \\ L^T G^{i^T} & P \end{bmatrix} > 0 \qquad \forall i = 1, \dots, N_V \tag{3.34c}$$

To sum up, if such P and L exist, then the control law (3.17) with $K = LP^{-1}$ guarantees asymptotic stability to the closed-loop system for all possible parametrizations of the model compatible with the available data and similar closed-loop behavior with respect to reference model.

3.4.1.5 Algorithm

In this section, we present the algorithm used for the tuning of the regulator parameters.

The steps of the algorithm for Case I are the following:

1. Collect a dataset $\mathcal{D}$ with an open-loop experiment, select the reference model M and the inflation parameter α, and provide the maximum value for the bounded additive noise $\bar{d}$
2. Compute the global error bound estimation $\hat{\bar{\varepsilon}}$ with $\mathcal{D}$ and $\bar{d}$ by following the procedure as discussed in Section 2.3.4.

3. Find the N_V vertives of the feasible parameter set (FPS) $\widetilde{\Theta}$ as in Section 2.3.5 and construct the corresponding state-space models (F^i,G^i pairs) according to Section 3.2 for $i = 1, \dots, N_V$
4. Compute $y^o(k)$, construct $\mathbb{u}_1^\circ$ and $\mathbb{x}_1^\circ$, and compute the pseudo inverse matrix $\mathbb{x}_1^{\circ +}$
5. Solve the optimization problem in (3.34)
6. Set the parameter vector $K = LP^{-1}$ in case a feasible solution.

3.4.2 Case II: state-feedback controller with unknown system gain

In this part, the control design with closed-loop stability guarantees and desired closed-loop performance is derived when the system gain is unknown.

3.4.2.1 Proposed control scheme

The main objective in this part is coping with the unknown system gain. In order to achieve it, starting from the case considered in Section 3.4.1, a new control scheme is developed. The control law introduced in (3.17) can be restated as the following

$$u(k) = \rho y^o(k) - Kx^o(k) + Kx(k) \tag{3.35}$$

Since the system gain ρ is unknown, the control law can be restated as

$$u(k) = \gamma y^o(k) + Kx(k) \tag{3.36}$$

where γ is the necessary additional scalar unknown parameter to be tuned for compensating for the unknown gain.

The corresponding control system is depicted in Figure 3.4.

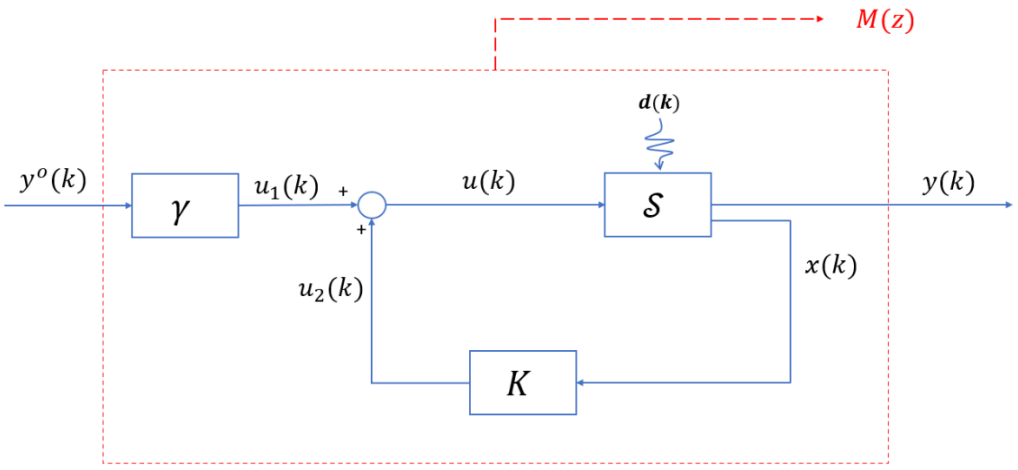

Figure 3.4: Block diagram in case the system gain is unknown

3.4.2.2 Closed-Loop model equations and stability condition

Considering the uncertain model $\mathcal{S}$ in equation (3.1) and the state-feedback control law in (3.36), the closed-loop dynamic equation can be obtained as

$$x(k+1) = F^{\circ}x(k) + G^{\circ}(\gamma y^{o}(k) + Kx(k)) + G_{w}w(k) \tag{3.37}$$

By means of simple computations, it can be rewritten as follows

$$x(k+1) = (F^{\circ} + G^{\circ}K)x(k) + G^{\circ}\gamma y^{o}(k) + G_{w}w(k) \tag{3.38}$$

According to dynamic equation above, the closed-loop Schur stability is provided in case of $\exists P = P^{T} > 0$ and K such that (3.15) holds for all $i = 1, \dots, N_{V}$.

3.4.2.3 VRFT cost function

The following VRFT cost function can be defined for any state-feedback controller parameter vector K and scalar parameter γ

$$J_{2}(K,\gamma) = \sum_{k=1}^{N-n_{r}} (u(k) - \mu y^{o}(k) - Kx(k))^{2} \tag{3.39}$$

The VRFT cost function can be reorganized as follows

$$J_{2}(K,\gamma) = \sum_{k=1}^{N-n_{r}} \left(u(k) - [y^{o}(k) \quad x^{T}(k)] \begin{bmatrix} \gamma \\ K^{T} \end{bmatrix}\right)^{2} \tag{3.40}$$

where $y^{o}(k)$ is the virtual reference and, according to Figure 3.4, we request to have the following relation

$$y^{o}(k) = M^{-1}(z)y(k) \tag{3.41}$$

The VRFT cost function in (3.40) can be written as

$$J_{2}(K,\gamma) = \left\| \mathbb{u}_{2}^{\circ} - \mathbb{x}_{2}^{\circ} \begin{bmatrix} \gamma \\ K^{T} \end{bmatrix} \right\|^{2} \tag{3.42}$$

where

$$\mathbb{u}_{2}^{\circ} = \begin{bmatrix} u(1) \\ \vdots \\ u(N-n_{r}) \end{bmatrix} \tag{3.43}$$

$$\mathbb{x}_2^\circ = \begin{bmatrix} y^o(1) & x^T(1) \\ \vdots & \vdots \\ y^o(N-n_r) & x^T(N-n_r) \end{bmatrix}$$

Remarkably, in the unconstrained case the solution of (3.42) is the following

$$\begin{bmatrix} \gamma \\ K^T \end{bmatrix} = \mathbb{x}_2^{\circ +} \mathbb{u}_2^\circ \tag{3.44}$$

Where $\mathbb{x}_2^{\circ +}$ is the pseudo-inverse of $\mathbb{x}_2^\circ$. This expression motivates the alternative cost function, which allows us to have an optimization problem in the variables P and L.

$$J_{22}(\gamma, P, L) = \left\| \mathbb{x}_2^{\circ +} \mathbb{u}_2^\circ - \begin{bmatrix} \gamma \\ K^T \end{bmatrix} \right\|^2_{\begin{bmatrix} 1 & 0 \\ 0 & P \end{bmatrix}} \tag{3.45}$$

where

$$K = LP^{-1} \tag{3.46}$$

We can obtain from (3.45) the following

$$\begin{aligned} J_{22}(\gamma, P, L) = (\mathbb{x}_2^{\circ +} \mathbb{u}_2^\circ)^T \begin{bmatrix} 1 & 0 \\ 0 & P \end{bmatrix} \mathbb{x}_2^{\circ +} \mathbb{u}_2^\circ - \left(\mathbb{x}_2^{\circ +} \mathbb{u}_2^\circ\right)^T \begin{bmatrix} 1 & 0 \\ 0 & P \end{bmatrix} \begin{bmatrix} \gamma \\ P^{-1}L^T \end{bmatrix} \\ - [\gamma \quad LP^{-1}] \begin{bmatrix} 1 & 0 \\ 0 & P \end{bmatrix} \mathbb{x}_2^{\circ +} \mathbb{u}_2^\circ + [\gamma \quad L] \begin{bmatrix} 1 & 0 \\ 0 & P^{-1} \end{bmatrix} \begin{bmatrix} \gamma \\ L^T \end{bmatrix} \end{aligned} \tag{3.47}$$

We can introduce a scalar σ that verify (3.47) in order to introduce an equivalent minimization problem to J_{22}

$$\min_{\sigma, \gamma, P, L} \sigma \tag{3.48a}$$

s.t.

$$\begin{aligned} \sigma - \left(\mathbb{x}_2^{\circ +} \mathbb{u}_2^\circ\right)^T \begin{bmatrix} 1 & 0 \\ 0 & P \end{bmatrix} \mathbb{x}_2^{\circ +} \mathbb{u}_2^\circ + \left(\mathbb{x}_2^{\circ +} \mathbb{u}_2^\circ\right)^T \begin{bmatrix} 1 & 0 \\ 0 & P \end{bmatrix} \begin{bmatrix} \gamma \\ P^{-1}L^T \end{bmatrix} \\ + [\gamma \quad LP^{-1}] \begin{bmatrix} 1 & 0 \\ 0 & P \end{bmatrix} \mathbb{x}_2^{\circ +} \mathbb{u}_2^\circ - [\gamma \quad L] \begin{bmatrix} 1 & 0 \\ 0 & P^{-1} \end{bmatrix} \begin{bmatrix} \gamma \\ L^T \end{bmatrix} \geq 0 \end{aligned} \tag{3.48b}$$

The Schur complement of (3.48) is given as follows

$$\begin{bmatrix} \sigma - \left(\mathbb{x}_2^{\circ +} \mathbb{u}_2^\circ\right)^T \begin{bmatrix} 1 & 0 \\ 0 & P \end{bmatrix} \mathbb{x}_2^{\circ +} \mathbb{u}_2^\circ + 2\left(\mathbb{x}_2^{\circ +} \mathbb{u}_2^\circ\right)^T \begin{bmatrix} \gamma \\ L^T \end{bmatrix} & [\gamma \quad L] \\ \begin{bmatrix} \gamma \\ L^T \end{bmatrix} & \begin{bmatrix} 1 & 0 \\ 0 & P \end{bmatrix} \end{bmatrix} \geq 0 \tag{3.49}$$

3.4.2.4 VRFT-based optimization problem with stability guarantees

Based on the VRFT-based cost function in the Section 3.4.2.3 and the closed-loop stability condition which can be also stated in terms of LMIs as shown in Section 3.4.2.2, we are now in the position to introduce the main optimization problem that allows to enforce VRFT-like performances and, at the same time, to guarantee robust stability of the closed loop system:

$$\min_{\sigma,\gamma,P,L} \sigma \tag{3.50a}$$

s.t.

$$\begin{bmatrix} \sigma - \left(\mathbb{x}_2^{\circ +} \mathbb{u}_2^{\circ}\right)^T \begin{bmatrix} 1 & 0 \\ 0 & P \end{bmatrix} \mathbb{x}_2^{\circ +} \mathbb{u}_2^{\circ} + 2\left(\mathbb{x}_2^{\circ +} \mathbb{u}_2^{\circ}\right)^T \begin{bmatrix} \gamma \\ L^T \end{bmatrix} & [\gamma \quad L] \\ \begin{bmatrix} \gamma \\ L^T \end{bmatrix} & \begin{bmatrix} 1 & 0 \\ 0 & P \end{bmatrix} \end{bmatrix} \geq 0 \tag{3.50b}$$

$$\begin{bmatrix} P - F^i P F^{i^T} - F^i L^T G^{i^T} - G^i L F^{i^T} & G^i L \\ L^T G^{i^T} & P \end{bmatrix} > 0 \tag{3.50c}$$

$$\forall i = 1, \dots, N_V$$

If such P and L exist, then the control law $K = LP^{-1}$ guarantees the asymptotic stability of the closed-loop system for all possible parametrizations of the model compatible with the available data and a similar closed-loop behavior with respect to the reference model.

Remarkably, to have better steady-state performance, a further additional step is required. In this step, we retune the scalar γ with the known K vector obtained in (3.50). The corresponding additional step can be written as the following cost function J_2^* where the new optimum scalar gain is denoted with γ^*

$$\gamma^* = \underset{\tilde{\gamma}}{\operatorname{argmin}} J_2^*(\tilde{\gamma}) = \left\| \mathbb{x}_2^{\circ +} \mathbb{u}_2^{\circ} - \begin{bmatrix} \tilde{\gamma} \\ K \end{bmatrix} \right\|^2 \tag{3.51}$$

3.4.2.5 Algorithm

In this section, we derive the algorithm for the parameter tuning procedure.

The steps of the algorithm for Case II are the following

1. Collect a dataset $\mathcal{D}$ with an open-loop experiment, select the reference model M and the inflation parameter α, and provide the maximum value for the bounded additive noise $\bar{d}$
2. Compute the global error bound estimation $\hat{\bar{\varepsilon}}$ (with $\mathcal{D}$ and $\bar{d}$) by following the procedure as discussed in Section 2.3.4.
3. Find the N_V vertices of the Feasible Parameter Set (FPS) $\widetilde{\Theta}$ as in Section 2.3.5 and construct the corresponding state-space models (F^i,G^i pairs) according to Section 3.2 for $i = 1, \dots, N_V$
4. Compute $y^o(k)$, construct $\mathbb{U}_2^\circ$ and $\mathbb{X}_2^\circ$, and compute the pseudo-inverse matrix $\mathbb{X}_2^{\circ +}$
5. Solve the optimization problem in (3.50)
6. Set the parameter vector $K = LP^{-1}$ in case a feasible solution.
7. Set $\gamma = \gamma^*$ after performing (3.51)

3.4.3 Case III: integrator

In this part, we investigate the regulator with closed-loop stability guarantees and desired closed-loop performance in case the controller is equipped with an explicit integrator.

3.4.3.1 Proposed control scheme

Considering the uncertain model $\mathcal{S}$ in equation (3.1), we consider the control scheme depicted in Figure 3.5.

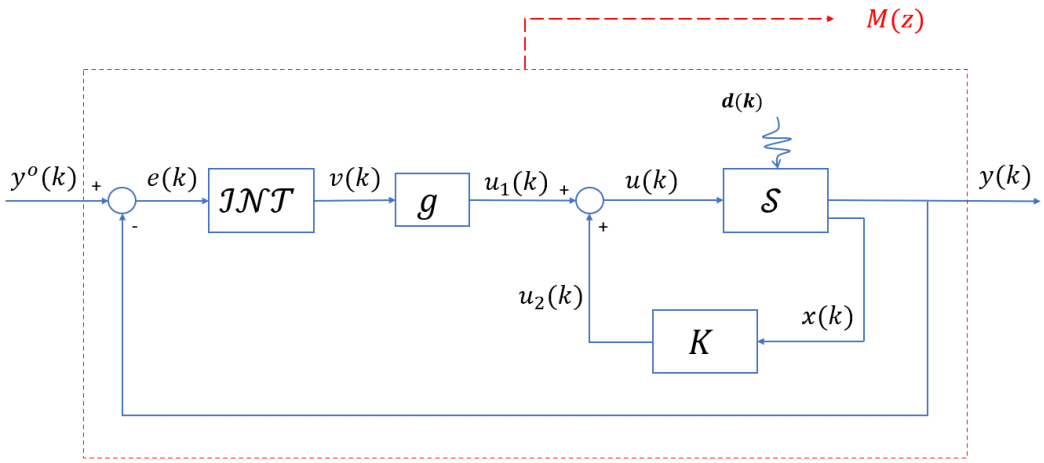

Figure 3.5: Block diagram in case of controller equipped with explicit integrator

According to Figure 3.5, the control law can be defined using the following state-space realization

$$\begin{cases} \eta(k+1) = \eta(k) + e(k) \\ u(k) = Kx(k) + g\big(\eta(k) + e(k)\big) \end{cases} \tag{3.52}$$

3.4.3.2 Closed-loop model equations and the stability condition

The closed-loop dynamic equation with the state-feedback controller (3.52) is

$$\begin{aligned} x(k+1) &= F^{\circ}x(k) + G^{\circ}\Big(Kx(k) + g\big(\eta(k) - Hx(k)\big)\Big) \\ \eta(k+1) &= \eta(k) - Hx(k) \end{aligned} \tag{3.53}$$

where g is the additional scalar parameter to be tuned together with vector K. Note that, since the reference signal $y^o(k)$ and the signal $w(k)$ do not affect the stability, they are neglected in (3.53). In the light of this fact, the error term in (3.53) can described by $-y(k) = -Hx(k)$.

The alternative closed-loop system dynamics can be rewritten as the following state-space realization by defining the new state variable $\zeta(k) = [x(k)^T \quad \eta(k)]^T$

$$\zeta(k+1) = D^o\zeta(k) \tag{3.54}$$

where

$$D^o = \begin{bmatrix} F^o + G^oK - gG^oH & gG^o \\ -H & 1 \end{bmatrix} \tag{3.55}$$

$D^o = A^o + B^oJ$ can be rewritten as the following

$$D^o = \begin{bmatrix} F^o & 0_{(n_a+n_b-1)\text{x}1} \\ -H & 1 \end{bmatrix} + \begin{bmatrix} G^o \\ 0 \end{bmatrix} [K - gH \quad g] \tag{3.56}$$

where $A^o = \begin{bmatrix} F^o & 0_{(n_a+n_b-1)\text{x}1} \\ -H & 1 \end{bmatrix}$, $B^o = \begin{bmatrix} G^o \\ 0 \end{bmatrix}$ and $J = [K - gH \quad g]$. Moreover, the following further decomposition is required in order to have parameters directly in one vector

$$[K \quad g] = JE^{-1} \tag{3.57}$$

where

$$E = \begin{bmatrix} I_{(n_a+n_b-1)} & 0_{(n_a+n_b-1)\text{x}1} \\ -H & 1 \end{bmatrix} \tag{3.58}$$

Notably, (3.9) is also valid for the pair A^o and B^o and the following relation is verified for $i = 1, \dots, N_V$

$$[A^o \quad B^o] = \sum_{i=1}^{N_V} \lambda_i \, [A^i \quad B^i] \tag{3.59}$$

Note that, an alternative robust stability condition considered for Case III. The derivation of a condition for robust stability in terms of LMIs is shown step by step starting from verifying the Schur stability of the closed-loop system.

Considering the closed-loop system given in (3.54), the Schur stability of D^o is guaranteed if $\exists P = P^T > 0$ and $t > 0$ such that

$$D^{oT} P^{-1} D^o - P^{-1} + t I_{(n_a+n_b)} \leq 0 \tag{3.60}$$

Consistently, (3.60) holds if and only if $\exists P = P^T > 0$ such that

$$P\left(D^{oT} P^{-1} D^o - P^{-1} + t I_{(n_a+n_b)}\right) P \leq 0 \tag{3.61}$$

After substituting $D^o = A^o + B^o J$ and basic computations, (3.61) can be rewritten as follows

$$P - [P \quad (A^o P + B^o L)^T] \begin{bmatrix} t I_{(n_a+n_b)} & 0_{(n_a+n_b)\text{x}(n_a+n_b)} \\ 0_{(n_a+n_b)\text{x}(n_a+n_b)} & P^{-1} \end{bmatrix} \begin{bmatrix} P \\ A^o P + B^o L \end{bmatrix} \geq 0 \tag{3.62}$$

where $L = JP$. In view of the Schur complement, (3.62) is equivalent the following LMI

$$\begin{bmatrix} P & P & (A^o P + B^o L)^T \\ P & t^{-1} I_{(n_a+n_b)} & 0_{(n_a+n_b)\text{x}(n_a+n_b)} \\ (A^o P + B^o L) & 0_{(n_a+n_b)\text{x}(n_a+n_b)} & P \end{bmatrix} \geq 0 \tag{3.63}$$

Considering (3.59), if $\exists P = P^T > 0$ and L such that for $i = 1, \dots, N_V$ and $t > 0$ (3.63) holds, then the closed-loop asymptotic stability for (3.54) is guaranteed for $[K \quad g] = LP^{-1}E^{-1}$.

3.4.3.3 VRFT cost function

The following VRFT cost function can be defined for any state-feedback controller parameter vector K and scalar parameter g

$$J_3(K,g) = \sum_{k=1}^{N-n_r} \left(u(k) - \begin{bmatrix} K & g \end{bmatrix} \begin{bmatrix} x(k) \\ \bar{v}(k) \end{bmatrix} \right)^2 \tag{3.64}$$

where $y^o(k)$ is the virtual reference and $\bar{v}(k)$ the integrated virtual error. The virtual reference $y^o(k)$ can be derived from $y(k)$ according to Figure 3.5, by computing

$$y^o(k) = M^{-1}(z)y(k) \tag{3.65}$$

On the other hand, after obtaining the virtual reference, the integrated error $\bar{v}(k)$ can be derived by computing recursively the equation set listed below

$$\bar{e}(k) = y^o(k) - y(k) \tag{3.66a}$$

$$\bar{v}(k) = \bar{v}(k-1) + \bar{e}(k) \tag{3.66b}$$

The VRFT cost function in (3.64) can be written in a more compact form as

$$J_3(K,g) = \left\| \mathbb{u}_3^\circ - \mathbb{x}_3^\circ E^{-T} J^T \right\|^2 \tag{3.67}$$

where

$$\begin{aligned} \mathbb{u}_3^\circ &= \begin{bmatrix} u(1) \\ \vdots \\ u(N-n_r) \end{bmatrix} \\ \mathbb{x}_3^\circ &= \begin{bmatrix} x^T(1) & \bar{v}(1) \\ \vdots & \vdots \\ x^T(N-n_r) & \bar{v}(N-n_r) \end{bmatrix} \end{aligned} \tag{3.68}$$

Note that, by considering (3.57), minimizing (3.67) leads to the following solution in the unconstrained case,

$$\begin{bmatrix} K & g \end{bmatrix}^T = \mathbb{x}_3^{\circ +} \mathbb{u}_3^\circ \tag{3.69}$$

where $\mathbb{x}_3^{\circ +}$ is the pseudo-inverse of $\mathbb{x}_3^\circ$. At this point, we define the following alternative cost function J_{32} compatible with a reformulation as an LMI optimization problem in the variables P and L based on (3.67).

$$J_{32}(L,P) = \left\| E^T \mathbb{x}_3^{\circ +} \mathbb{u}_3^\circ - J^T \right\|_P^2 \tag{3.70}$$

where

$$L = JP \tag{3.71}$$

The cost function J_{32} in equation (3.70) can be rewritten as

$$\begin{aligned} J_{32}(L,P) = \mathbb{u}_3^{\circ T}(E^T\mathbb{x}_3^{\circ +})^T P E^T \mathbb{x}_3^{\circ +}\mathbb{u}_3^{\circ} + LP^{-1}L^T \\ - \mathbb{u}_3^{\circ T}\left(E^T\mathbb{x}_3^{\circ +}\right)^T L^T - LE^T\mathbb{x}_3^{\circ +}\mathbb{u}_3^{\circ} \end{aligned} \tag{3.72}$$

Note that, minimizing J_{32} is equivalent to minimizing a scalar σ such that

$$\sigma - \mathbb{u}_3^{\circ T}(E^T\mathbb{x}_3^{\circ +})^T P E^T \mathbb{x}_3^{\circ +}\mathbb{u}_3^{\circ} - LP^{-1}L^T + 2\mathbb{u}_3^{\circ T}(E^T\mathbb{x}_3^{\circ +})^T L^T \geq 0 \tag{3.73}$$

The latter inequality can be rewritten, thanks to the Schur complement, as

$$\begin{bmatrix} \sigma - \mathbb{u}_3^{\circ T}\left(E^T\mathbb{x}_3^{\circ +}\right)^T P E^T \mathbb{x}_3^{\circ +}\mathbb{u}_3^{\circ} + 2LE^T\mathbb{x}_3^{\circ +}\mathbb{u}_3^{\circ} & L \\ L^T & P \end{bmatrix} \geq 0 \tag{3.74}$$

3.4.3.4 VRFT-based optimization problem with stability guarantees

We have a VRFT-based cost function which is stated in terms of LMI as shown in Section 3.4.3.3 and the closed-loop stability condition which can be also stated in terms of LMIs as shown in Section 3.4.3.2. This motivates the following optimization problem that allows to enforce VRFT-like performances and, at the same time, to guarantee robust stability of the closed-loop system:

$$\min_{\sigma,P,L} \sigma \tag{3.75a}$$

s.t.

$$\begin{bmatrix} \sigma - \mathbb{u}_3^{\circ T}\left(E^T\mathbb{x}_3^{\circ +}\right)^T P E^T \mathbb{x}_3^{\circ +}\mathbb{u}_3^{\circ} + 2LE^T\mathbb{x}_3^{\circ +}\mathbb{u}_3^{\circ} & L \\ L^T & P \end{bmatrix} \geq 0 \tag{3.75b}$$

$$\begin{bmatrix} P & P & (A^iP + B^iL)^T \\ P & t^{-1}I_{(n_a+n_b)} & 0_{(n_a+n_b)\mathrm{x}(n_a+n_b)} \\ (A^iP + B^iL) & 0_{(n_a+n_b)\mathrm{x}(n_a+n_b)} & P \end{bmatrix} \geq 0 \tag{3.75c}$$

$$\forall i = 1, \dots, N_V, with\ t > 0$$

To sum up, if such P and L exist, then the control law (3.52) with $[K \quad g] = LP^{-1}E^{-1}$ guarantees asymptotic stability for the closed-loop system for all possible parametrizations of the model compatible with the available data and similar closed-loop behavior with respect to reference model.

3.4.3.5 Algorithm

In this section, we present the algorithm for the parameter tuning.

The steps of the algorithm for Case III are the following

1. Collect a dataset $\mathcal{D}$ with an open-loop experiment, select the reference model M and the inflation parameter α, and provide a positive scalar t and the maximum value for the bounded additive noise $\bar{d}$
2. Compute the global error bound estimation $\hat{\bar{\varepsilon}}$
3. with $\mathcal{D}$ and $\bar{d}$ by following the procedure as discussed in Section 2.3.4.
4. Find the N_V vertices of Feasible Parameter Set (FPS) $\widetilde{\Theta}$ as in Section 2.3.5 and the state-space models (A^i,B^i pairs) according to (3.56) and (3.59) by using (3.10) for $i = 1, \dots, N_V$
5. Compute $y^o(k)$ and $\bar{v}(k)$, construct E, $\mathbb{U}_3^\circ$ and $\mathbb{X}_3^\circ$, and compute the pseudo-inverse matrix $\mathbb{X}_3^{\circ +}$
6. Solve the optimization problem (3.75)
7. Set the parameter vector $[K \quad g] = LP^{-1}E^{-1}$ in case a feasible solution.

4. Simulation example

In this chapter, the data-driven methods proposed in Chapter 3 for control of unknown linear systems with robust closed-loop stability guarantees are validated on a simulation example in the MATLAB/Simulink environment.

4.1 Mathematical model

We consider the system illustrated in Figure 4.1, consisting of a cascade interconnection of three tanks: u_1 is the input flowrate, while h_i corresponds to the water level each reservoir, $i = 1,2,3$.

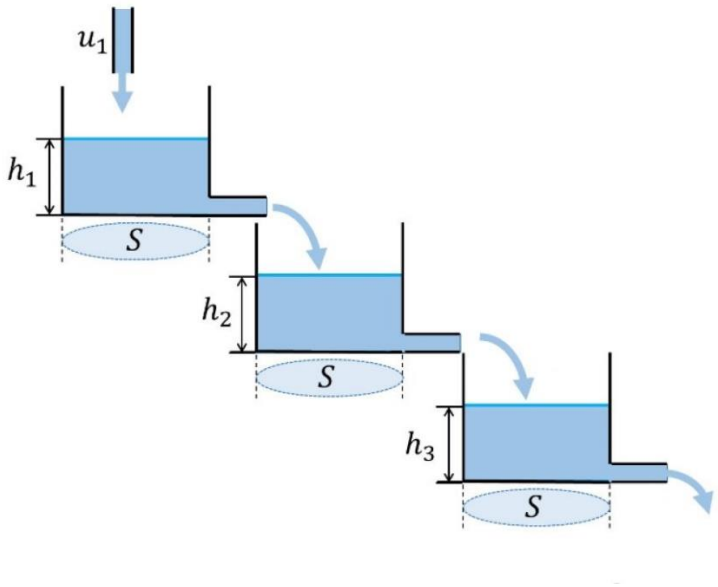

Figure 4.1: Three cascaded tanks system

The corresponding linearized centralized model is the following

$$\begin{cases} S\dot{h}_1 = -kh_1 + u_1 \\ S\dot{h}_2 = kh_1 - kh_2 \\ S\dot{h}_3 = kh_2 - kh_3 \end{cases} \tag{4.1}$$

where $S = 1\,m^2$ and $k = 1\ {}^{m^2}/_{s}$. Note that, since the model is linearized around a nominal condition, all the variables of the model should be regarded as differences with respect to the nominal values. We assume that all levels are measurable. Defining

$\hat{x} = [h_1 \quad h_2 \quad h_3]^T$ and $u = u_1$, the system dynamics is described by the following model

$$\dot{\hat{x}} = \begin{bmatrix} -1 & 0 & 0 \\ 1 & -1 & 0 \\ 0 & 1 & -1 \end{bmatrix} \hat{x} + \begin{bmatrix} 1 \\ 0 \\ 0 \end{bmatrix} u \tag{4.2}$$

4.2 Process implementation

We define the plant considering u_1 as input and h_3 as output. The plant transfer function can be written as follows

$$G(s) = \frac{Y(s)}{U(s)} = \frac{1}{(s+1)^3} = \frac{1}{s^3 + 3s^2 + 3s + 1} \tag{4.3}$$

The system is discretized with a sampling time T_s of 0.5 s with the Zero Order Hold method and the corresponding discrete-time transfer function is

$$\frac{Y(z)}{U(z)} = \frac{0.01439z^{-1} + 0.03973z^{-2} + 0.006794z^{-3}}{1 - 1.82z^{-1} + 1.104z^{-2} - 0.2231z^{-3}} \tag{4.4}$$

In Figure 4.2, the open-loop step responses of the system can be observed.

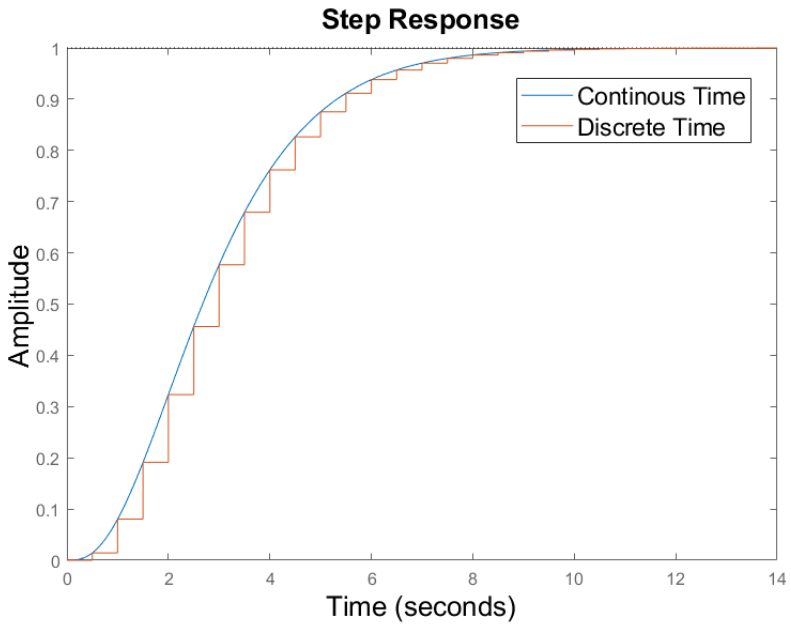

Figure 4.2: Open-loop step responses in discrete and continuous time

Note that, for a more realistic simulation, the output measurement is corrupted by an additional random noise. Therefore, the system in equation (4.4) can be rewritten as the following difference equation form, as done in (3.5) where $w(k)$ is responsible for the noise effect and prediction error

$$\begin{aligned} y(k) = {} & 1.82y(k-1) - 1.104y(k-2) + 0.2231y(k-3) \\ & + 0.01439u(k-1) + 0.03973u(k-2) \\ & + 0.006794u(k-3) + w(k) \end{aligned} \tag{4.5}$$

By taking into consideration the state-space realization in Chapter 3, the states can be defined as

$$x(k) = \begin{bmatrix} y(k) \\ y(k-1) \\ y(k-2) \\ u(k-1) \\ u(k-2) \end{bmatrix} \tag{4.6}$$

Furthermore, bearing in mind that θ^o is the real parameter vector and defined as $\theta^o = [1.82 \quad -1.104 \quad 0.2231 \quad 0.01439 \quad 0.03973 \quad 0.006794]^T$, the state-space matrices for the real system

$$\begin{cases} x(k+1) = F^o x(k) + G^o u(k) + G_w w(k) \\ y(k) = Hx(k) \end{cases} \tag{4.7}$$

where

$$F^\circ = \begin{bmatrix} 1.82 & -1.104 & 0.2231 & 0.03973 & 0.006794 \\ 1 & 0 & 0 & 0 & 0 \\ 0 & 1 & 0 & 0 & 0 \\ 0 & 0 & 0 & 0 & 0 \\ 0 & 0 & 0 & 1 & 0 \end{bmatrix}_{5\times 5}$$

$$G^o = \begin{bmatrix} 0.01439 \\ 0 \\ 0 \\ 1 \\ 0 \end{bmatrix}, \qquad G_w = \begin{bmatrix} 1 \\ 0 \\ 0 \\ 0 \\ 0 \end{bmatrix} \tag{4.8}$$

$$H = [1 \quad 0 \quad 0 \quad 0 \quad 0]$$

4.3 Data collection

Since the proposed approach is a data-driven offline noniterative method, a batch of data is required. Moreover, the same dataset is used for the controller tuning procedure as well as for computation of the feasible parameter set (FPS).

The batch of data consists of 10000 input-output pairs collected with an open-loop experiment on the simulated system. The system is fed by a multilevel pseudo-random signal (MPRS) in order to have a proper excitement on the system. The amplitude of the input signal is uniformly selected in the range $[-1,1]$. Furthermore, the first half of the dataset has switching period of T_s, i.e., 0.5 s and the other half has switching period of $50T_s$, i.e., 25 s. The choice of two different frequencies allows for a better identification for both the fast dynamics and slow ones.

The output measurement is affected by a measurement noise which varies uniformly at each time step in the range [-0.005,0.005]. The corresponding signal to noise ratio (SNR) is 42.616 dB. The corresponding dataset is shown in Figure 4.3.

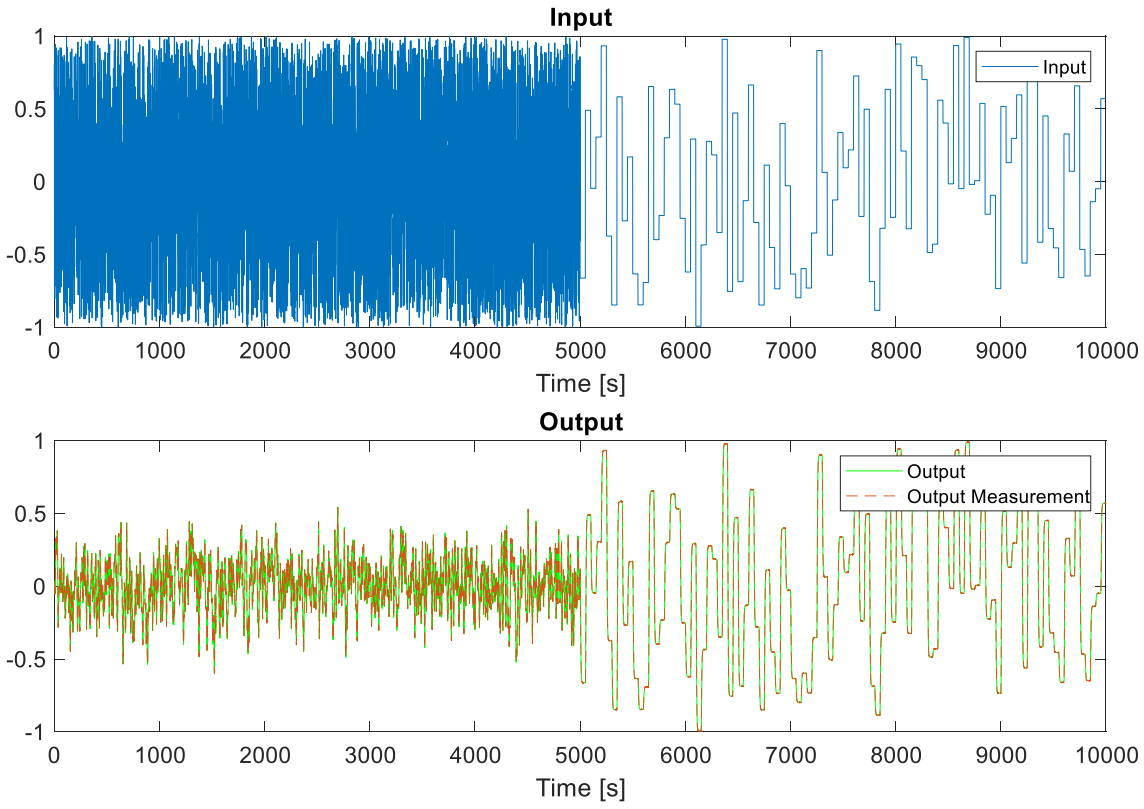

Figure 4.3: Input and output measurements of the open-loop experiment

4.4 Feasible parameter set (FPS)

According to equation (4.5), the regressor matrix can be obtained as follows

$$\varphi(k) = \begin{bmatrix} y(k-1) \\ y(k-2) \\ y(k-3) \\ u(k-1) \\ u(k-2) \\ u(k-3) \end{bmatrix} \tag{4.9}$$

The next step concerns the estimation of the global error bound. Therefore, the computation, (2.56) is performed with an inflation parameter α equal to 1.2. The corresponding global error bound estimation is found.

Thanks to the function *lcon2vert* [32] in MATLAB, the feasible parameter set $\widetilde{\Theta}$ is obtained with 3469 vertices. Since the number of parameters to be identified is a vector of six elements, the FPS is in a six-dimensional space. For the sake of graphical representation, the projections of the FPS in three-dimensional spaces are represented in Figure 4.4. Note that the real parameters are included in the FPS.

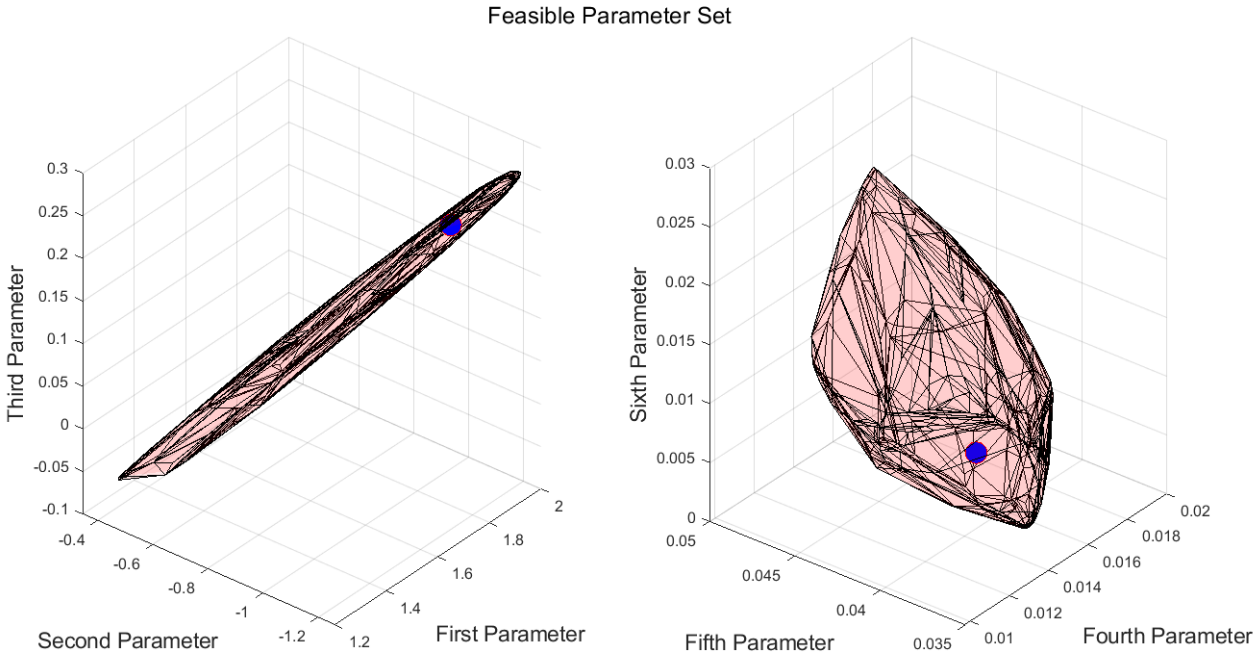

Figure 4.4: Feasible Parameter Set (blue spheres correspond to the real parameters)

4.5 Reference model

A reference model is selected, i.e.,

$$M(z) = \frac{0.4z^{-1}}{1 - 0.6z^{-1}} \tag{4.10}$$

In Figure 4.5, the open-loop response of the system and the reference model response for a step experiment are depicted. The open-loop response takes 18-time steps while the reference model takes 10-time steps to reach 1% settling time. It means we are expecting a much faster response.

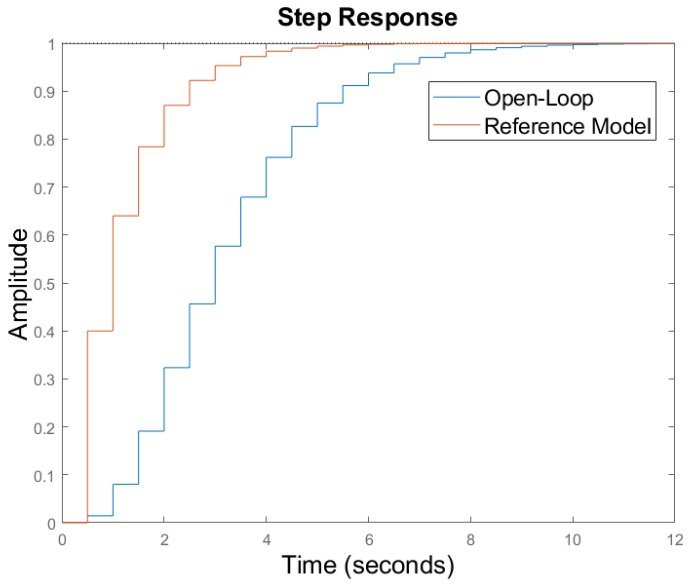

Figure 4.5: Step responses of open-loop system and reference model

Starting from (4.10), the following difference equation can be obtained

$$y(k) = 0.6y(k-1) + 0.4r(k-1) \tag{4.11}$$

In order to obtain the virtual reference, the following computation is required

$$r(k) = \frac{y(k+1) - 0.6y(k)}{0.4} \tag{4.12}$$

Since VRFT is solved offline, future output measurement values are available without any causality problem.

4.6 Validation

To evaluate the performances, the closed-loop results are compared with the desired closed-loop counterparts. The following performance index will be used

$$FIT(\%) = 100\left(1 - \frac{\|y - \hat{y}\|}{\|y - \bar{y}\|}\right) \tag{4.13}$$

where $\|\cdot\|$ denotes the Euclidean norm, y is the real system output vector, $\hat{y}$ is the desired output vector and $\bar{y}$ is the vector that has the same size with real system output vector and all elements of this vector are equal to the mean value of the real output vector.

Notably, since we are considering closed-loop stability, we considered another validation performance index, i.e., the spectral radius of the closed-loop system.

4.7 Simulation results

In this section we evaluate the reference tracking performance for each control scheme proposed in Chapter 3.

The validation phase of the closed-loop system is provided by a new experiment. In this experiment the reference signal used is specified for the following sections of the thesis in Table 4.1.

Reference	Interval
0	[0,20)
1	[20,40)
-1	[40,60)
2	[60,80)
1	[80,...]

Table 4.1: Reference input values

4.7.1 Case I

In this part we investigate the simulation results of the case where the system gain is assumed to be known (or a-priori identified).

Note that, by performing the algorithm discussed in Section 3.4.1.5, we can obtain the VRFT-based stability guarantees (SM-VRFT in Table 4.2). In order to compare the results with set membership approach (SM in Table 4.2) in which we only guarantee the closed-loop stability, we remove the terms (3.34a) and (3.34b). On the other hand, to obtain the solution to VRFT only (VRFT in Table 4.2) we perform (3.34) without (3.34c). However, it shouldn't be forgotten that there isn't any stability guarantee in the latter case.

The problem consists of 3470 Linear Matrix Inequalities. These LMIs are solved by minimizing the cost thanks to *YALMIP* [33] and the *MOSEK* [34] solvers in MATLAB.

Table 4.2 shows the spectral radius of the closed-loop systems and fit percentages computed as explained in Section 4.6.

As it can be seen from Table 4.2, VRFT alone cannot provide stability guarantees and therefore it is not represented in Figures 4.6 and 4.8.

	Spectral Radius $\rho(F)$	**Fit Percentage** $FIT(\%)$
VRFT	1.0194	-35.8908
SM	0.6214	70.2078
SM-VRFT	0.8409	93.3384

Table 4.2: The fit percentage and the spectral radius of closed-loop systems

According to Figure 4.6, we can see that SM provides stability for all possible plant parametrizations, and one of them is the real parameter vector. However, when the reference model similarity is taken into consideration, we can clearly see the effect of VRFT-based cost function. It provides quite similar closed loop behavior with respect to the reference model.

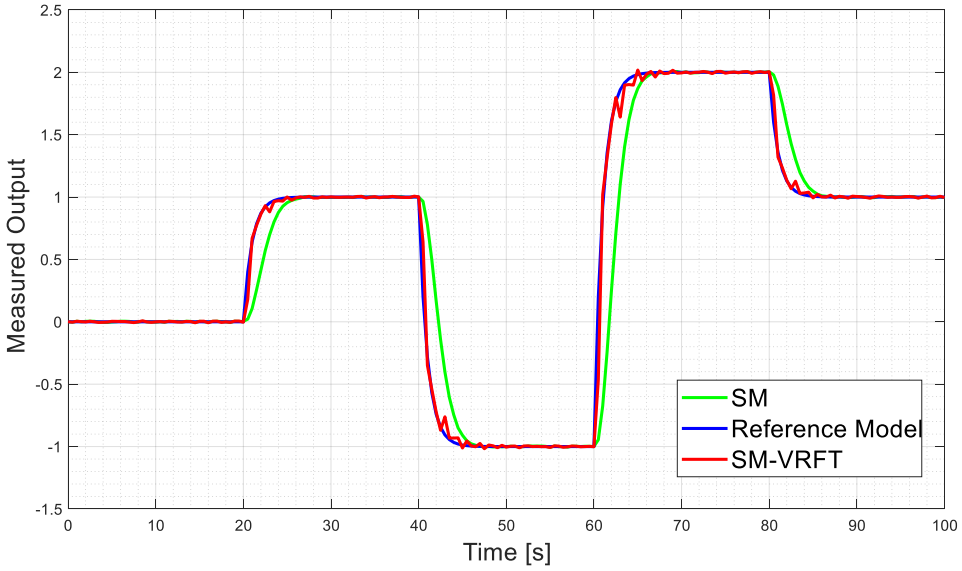

Figure 4.6: Output Trajectories of reference model, SM and SM-VRFT in Case I

Clearly, the trade-off for our case is between control effort and the desired performance. From Figure 4.7, the control variable for SM and SM-VRFT cases can be observed.

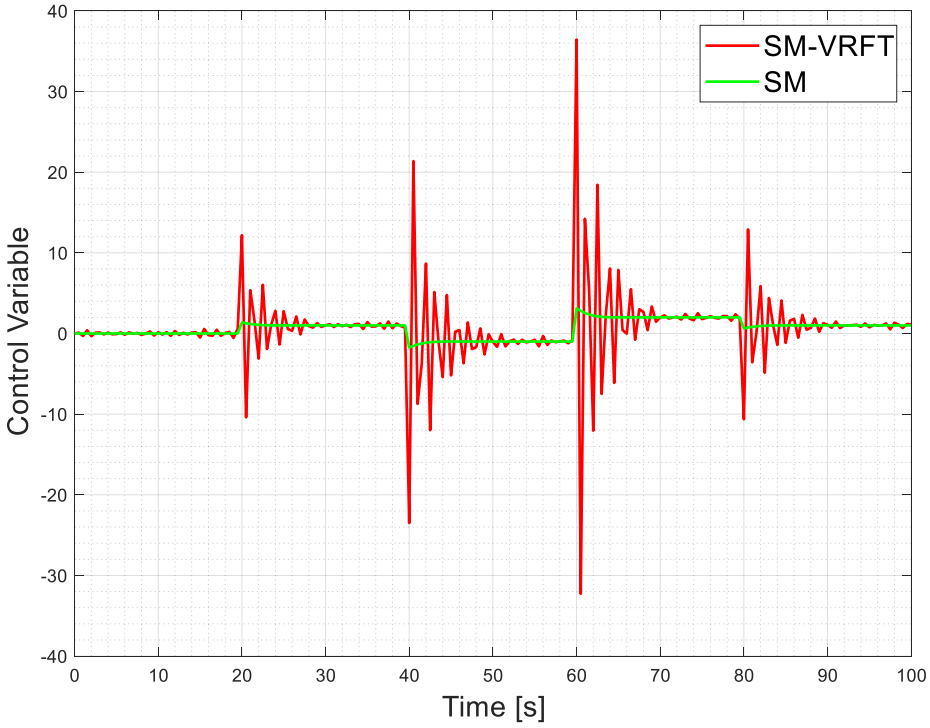

Figure 4.7: Input trajectories of SM and SM-VRFT in Case I

4.7.2 Case II

In this part we investigate the simulation results of the case where the system gain is unknown.

The tuning parameter are the state feedback gain $K = [K_1 \quad K_2 \quad K_3 \quad K_4 \quad K_5]^T$ and the static gain μ.

In MATLAB, *MOSEK* and *YALMIP* are used to solve VRFT-based stability guarantees optimization problem defined in Section 3.4.2.4. Yet, we consider three different cases as in the previous section. The spectral radius and fit percentages are presented in Table 4.3.

	Spectral Radius $\rho(F)$	**Fit Percentage** $FIT(\%)$
VRFT	1.0172	-2.0515
SM	0.6214	69.3997
SM-VRFT	0.8417	93.3437

Table 4.3: The fit percentage and the spectral radius of closed-loop systems

As it can be seen from Figure 4.8, SM alone cannot meet the correct steady-state position. However, SM-VRFT provides similar performances as in the previous case. VRFT cannot provide closed-loop stability.

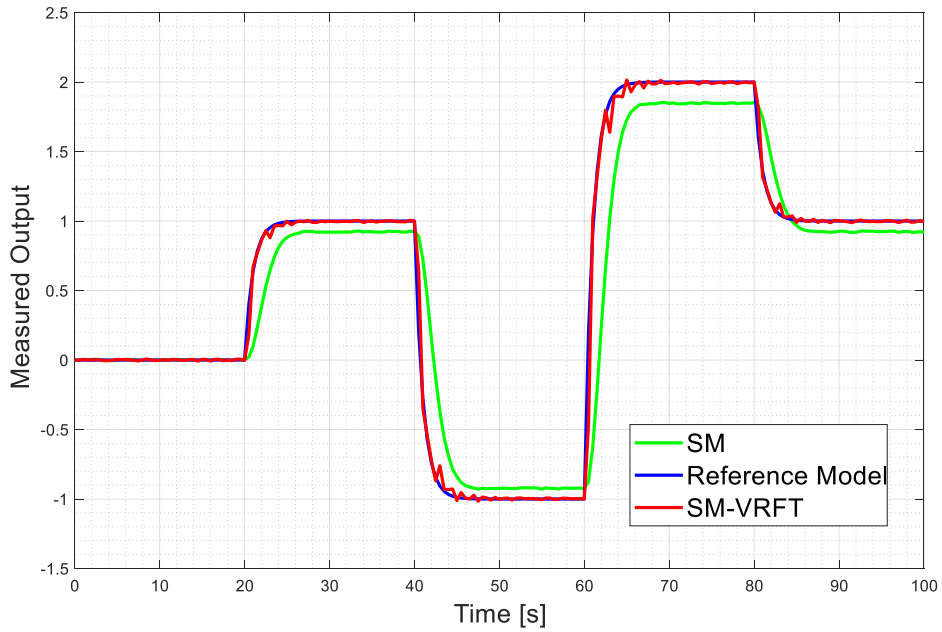

Figure 4.8: Output Trajectories of reference model, SM and SM-VRFT in Case II

According to Figure 4.9, we can observe that, similarly to Case I, to have desired closed-loop performance, a larger control effort is required.

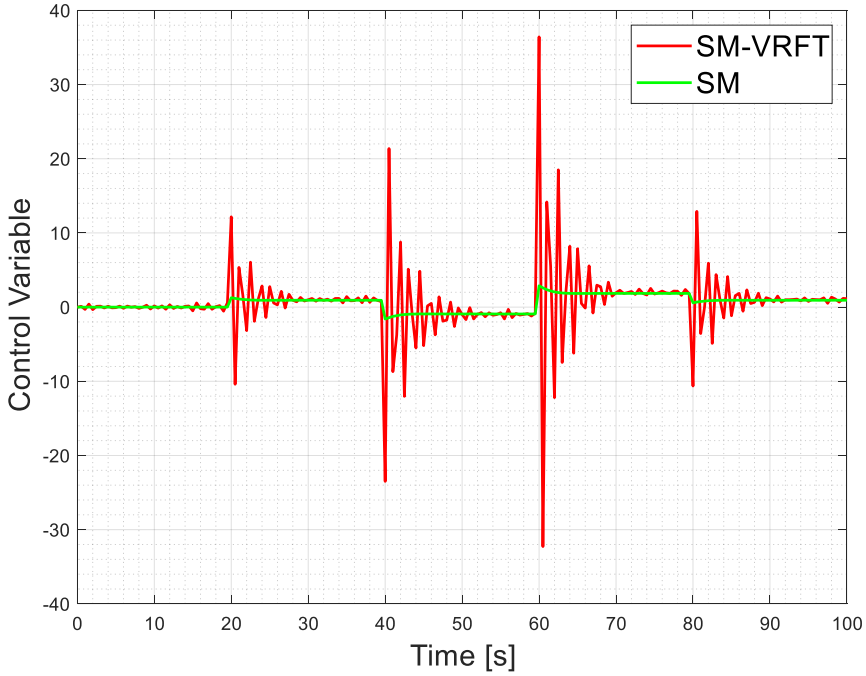

Figure 4.9: Input trajectories of SM and SM-VRFT in Case II

4.7.3 Case III

In this part, we investigate the simulation results in case an explicit integrator is embedded in the feedback system.

The parameter set to be tuned in Case III consists of the state feedback gain $K = [K_1 \quad K_2 \quad K_3 \quad K_4 \quad K_5]^T$ and the static integral gain g. Furthermore, we choose $t = 0.01$ s to solve the VRFT-based optimization problem proposed in Section 3.4.3.4.

According to Table 4.4, VRFT alone is not capable of providing closed-loop stability. On the other hand, SM-VRFT maintains closed-loop stability and has a better fit percentage. In Figure 4.10, the simulation results are shown.

	Spectral Radius $\rho(F)$	**Fit Percentage** $FIT(\%)$
VRFT	1.5147	-9.5e+33
SM	0.7306	69.0891
SM-VRFT	0.6935	76.0497

Table 4.4: The fit percentage and the spectral radius of closed-loop systems

With respect to Case I and Case II, we can observe that the output response is quite slow in Case III. On the other hand, the control effort is significantly smaller for Case III.

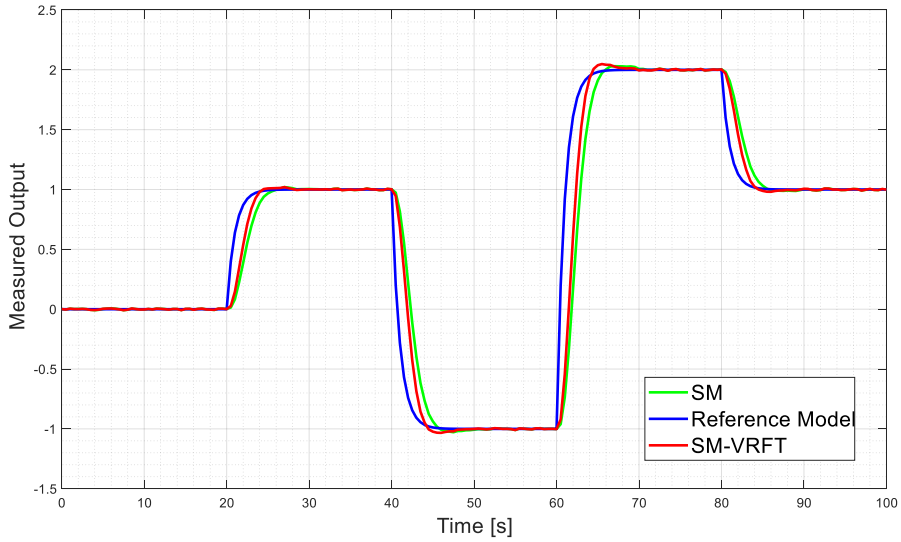

Figure 4.10: Output Trajectories of reference model, SM and SM-VRFT in Case III

Figure 4.11 displays the input trajectories for both cases. We can observe that the noise on the measured output induces the high frequency components even at steady-state.

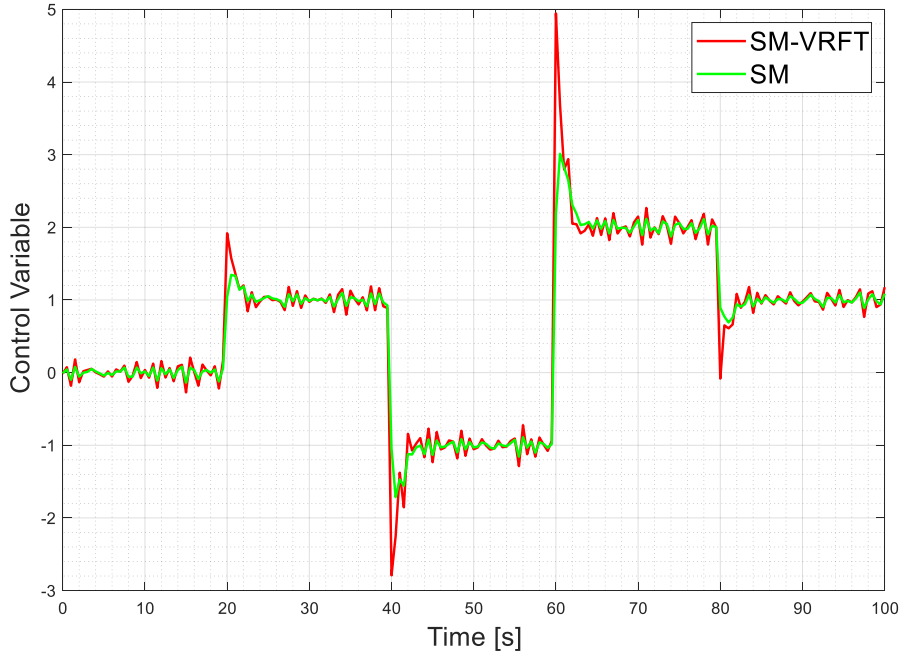

Figure 4.11: Input trajectories of SM and SM-VRFT in Case III

4.8 Comparison with direct control design based on controller unfalsification with stability guarantees

In this chapter, the results obtained applying the design methods proposed in Chapter 3 are compared with the ones obtained with the direct control design method introduced in Section 2.2. Both the approaches have the goal of achieving closed-loop stability and minimizing a model reference criterion, simultaneously. Moreover, both are data-driven noniterative offline methods.

In the following subsections they are compared different cases: when a first-order, a second-order reference model is considered. Also, we consider the case of a first-order reference model, but where experiments display a higher noise standard deviation, respectively.

4.8.1 First-order reference model

In this part we compare the approaches for the case with first-order reference model.

The direct control design based on controller unfalsification with stability guarantees approach is designed with the same dataset borrowed from Section 4.3.

The desired complementary sensitivity function $W(z)$ and the reference model $M(z)$ are expressed with the same first-order transfer function. The desired input sensitivity function $Q(z)$ is chosen under the assumption that the system gain is known.

$$W(z) = M(z) = \frac{0.4z^{-1}}{1 - 0.6z^{-1}} \tag{4.14a}$$

$$Q(z) = \frac{1}{\hat{P}(1)} \frac{(1 - 0.02z^{-1})}{1 - 0.6z^{-1}} \frac{0.4}{0.98} \tag{4.14b}$$

where $\hat{P}(1)$ is the estimated system gain, with $\hat{P}(1) = 1$.

The controller to be tuned for direct control design based on controller unfalsification with stability guarantees is parametrized as follows

$$\begin{aligned} C(z,\theta) = \frac{\bar{S}(z,\theta)S^*(z)}{\bar{R}(z,\theta)R^*(z)} &= \frac{1}{1 - z^{-1}} \frac{\bar{S}(z,\theta)}{\bar{R}(z,\theta)} \\ &= \frac{1}{1 - z^{-1}} \frac{s_0 + s_1 z^{-1} + s_2 z^{-2} + s_3 z^{-3}}{1 + r_1 z^{-1} + r_2 z^{-2} + r_3 z^{-3}} \end{aligned} \tag{4.15}$$

The simulation results are validated on reference-tracking experiment that has the consecutive steps listed in Table 4.5.

Reference	Interval
0	[0,20)
1	[20,40)
-1	[40,60)
2	[60,80)
1	[80,...]

Table 4.5: Reference input values

4.8.1.1 *Implementation of direct control design based on controller unfalsification with stability guarantees*

In this section we implement direct control design based on controller unfalsification with stability guarantees introduced in Section 2.2. $\mathcal{D}$ is the same dataset used in Section 4.3, $Q(z)$ and $W(z)$ are as in (3.14), the scalar $\tilde{\alpha} = 0.2$ is considered.

The optimal controller parameter vector $\theta_N = [s_0 \quad s_1 \quad s_2 \quad s_3 \quad r_1 \quad r_2 \quad r_3]$ is found by minimizing the related cost function. The *ga* function in MATLAB allows to find the optimum solution for a specified δ.

As the algorithm states, the first step is the computation of the cost function for $\delta = 0$ and after verifying the presence of the stability for this case, the largest δ is found. According to Table 4.6, $\delta = 0.8$ is the best solution since larger δ values fail on the algorithm.

	ETFE of $\|Q(d)\Delta_Q(\theta,d)\|_\infty$	Spectral Radius $\rho(F)$	Fit Percentage $FIT(\%)$
$\boldsymbol{\delta = 0}$	0.8232	0.8452	76.0008
$\boldsymbol{\delta = 0.8}$	0.9532	0.7616	78.5574
$\boldsymbol{\delta = 0.85}$	1.0687	0.8350	-
$\boldsymbol{\delta = 0.9}$	1.1023	0.9685	-
$\boldsymbol{\delta = 1}$	1.4707	1.0718	-

Table 4.6: The fit percentage, ETFE of $\|Q(d)\Delta_Q(\theta,d)\|_\infty$ and the spectral radius of closed-loop systems for different δ

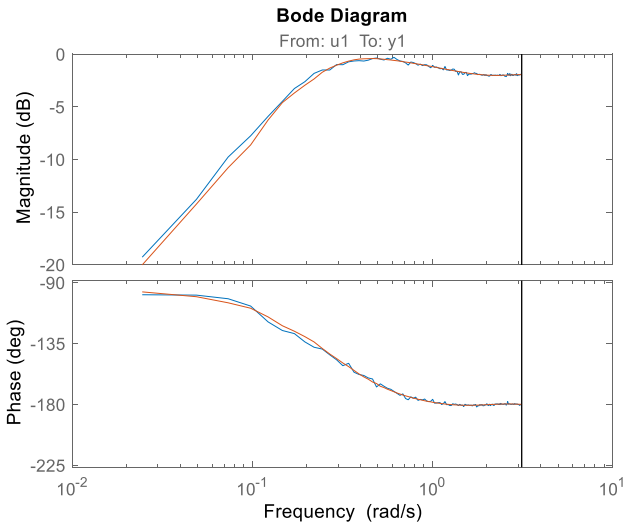

Figure 4.12: Bode diagram of ETFE of $\left\|Q(d)\Delta_Q(\theta,d)\right\|_\infty$ for $\delta = 0.8$ while its smoothed version is in red

The Empirical Transfer Function Estimation (ETFE) is obtained using the *etfe* function of MATLAB and each of the estimation is smoothed with a Hamming Window that yields frequency resolution of about $\pi/200$. In Figure 4.12, the Bode diagram of estimation and smoothed estimation is given in case $\delta = 0.8$.

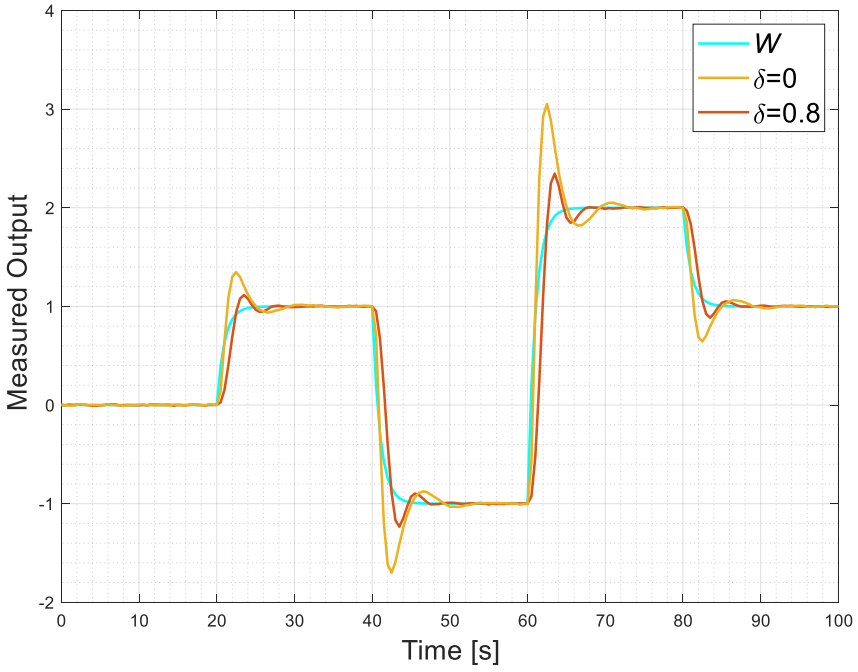

Figure 4.13: Output Trajectories of desired output sensitivity function, $\delta = 0.8$ and $\delta = 0$ cases

The output trajectories are depicted in Figure 4.13 for stability-guaranteed δ values. Moreover, in Figure 4.14, the input trajectories and the desired input sensitivity function response are shown.

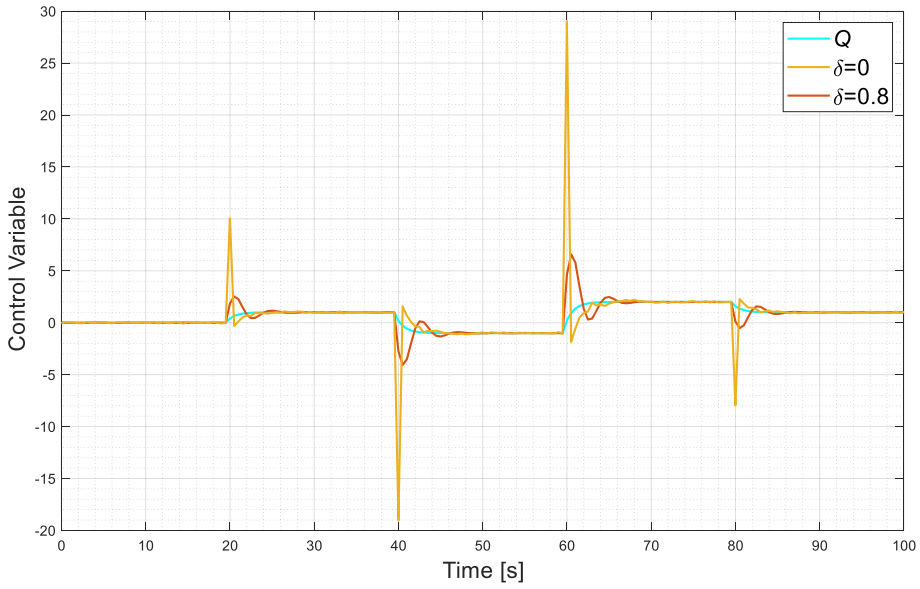

Figure 4.14: Input trajectories of desired input sensitivity function, $\delta = 0.8$ and $\delta = 0$ cases

4.8.1.2 *Comparison with the proposed approach*

In this section, the results obtained in Section 4.8.1.1 are compared with those obtained using the data-driven methods proposed in Chapter 3 for control of unknown linear systems with closed-loop stability guarantees.

Figure 4.15 and Figure 4.16 depict the input and output trajectories, respectively. Moreover, Table 4.7 displays the validation results. Case I and Case II display almost the same input and the output trajectories. They are more effective in following the reference model; however, this is done at the price of a more reactive control actions. On the other hand, Case III and the unfalsification method have smaller fit percentage, but the control effort required for these cases is smaller.

	Spectral Radius $\rho(F)$	**Fit Percentage** $FIT(\%)$
Case I	0.8409	93.3384
Case II	0.8417	93.3437
Case III	0.6935	76.0497

	ETFE of $\|Q(d)\Delta_Q(\theta,d)\|_\infty$	Spectral Radius $\rho(F)$	Fit Percentage $FIT(\%)$
$\boldsymbol{\delta = 0.8}$	0.9532	0.7616	78.5574

Table 4.7: Performance indexes for validation

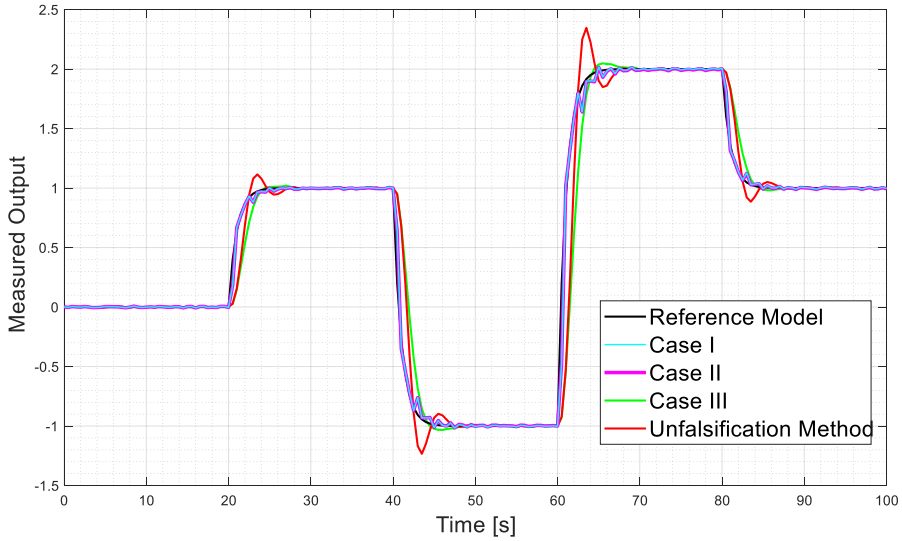

Figure 4.15: Output trajectories of Reference Model, Case I, Case II, Case III and UF with $\delta = 0.8$

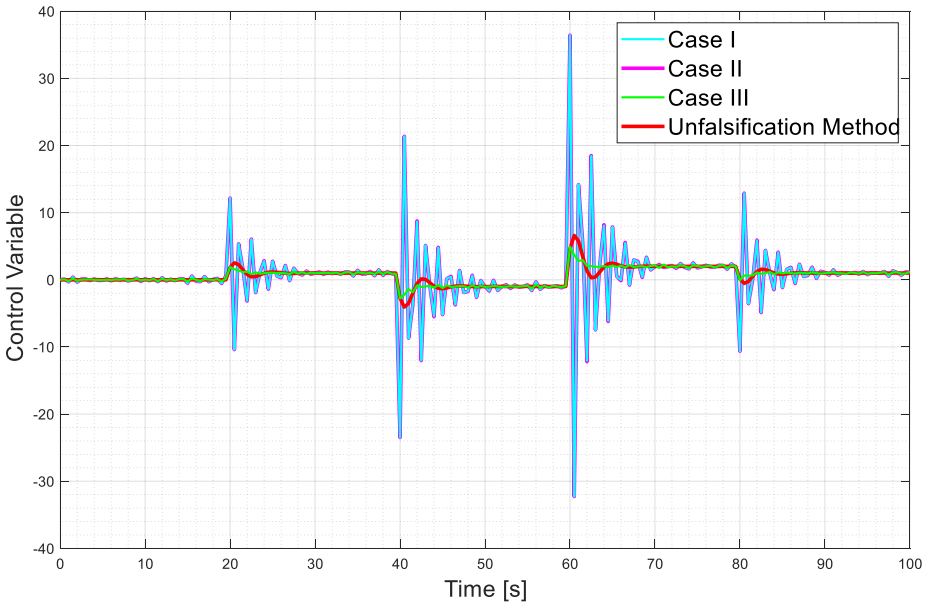

Figure 4.16: Input trajectories of Case I, Case II, Case III and UF with $\delta = 0.8$

4.8.2 Second-order reference models

In this part we compare the proposed approaches in case a second-order reference model choice is selected.

The desired complementary sensitivity function $W(z)$ and the reference model $M(z)$ consist of the same second-order transfer function. The desired input sensitivity function $Q(z)$ is also as a second-order transfer function sharing the denominator with others. Also note that by assuming that the estimated system gain is known, i.e., $\hat{P}(1) = 1$, $Q(z)$ is selected such that $W(1)= Q(1)\hat{P}(1)$.

The corresponding reference models are listed below

$$W(z) = M(z) = \frac{0.3325z^{-1} + 0.06481z^{-2}}{1 - 0.6067z^{-1} + 0.00404z^{-2}} \tag{4.16a}$$

$$Q(z) = \frac{10.22 - 16.67z^{-1} + 6.852z^{-2}}{1 - 0.6067z^{-1} + 0.00404z^{-2}} \tag{4.16b}$$

Notably, the desired output sensitivity function is quite similar to the one in (4.14a) but of second-order.

We design the controllers with the dataset collected in Section 4.3. Due to the fact that the reference models are changed, even if the FPS is preserved for the same dataset, the fictitious references are changed. Therefore, we reperform the data-driven control design of unknown linear systems with robust closed-loop stability guarantees for Case I, Case II and Case III with the available dataset.

4.8.2.1 Implementation of direct control design based on controller unfalsification with stability guarantees

In this section we implement the direct control design method discussed in Section 2.2.

Table 4.8 shows the validation performance indexes for three different values of δ. Moreover, to see the effect of δ, Figure 4.17 and Figure 4.18 are presented. The latter figures display the input and output trajectories compared with the ones obtained with the desired sensitivity functions.

	ETFE of $\|Q(d)\Delta_Q(\theta,d)\|_\infty$	Spectral Radius $\rho(F)$	Fit Percentage $FIT(\%)$
$\boldsymbol{\delta = 0}$	0.8060	0.9934	75.9311
$\boldsymbol{\delta = 0.99}$	0.7790	0.8079	91.0705
$\boldsymbol{\delta = 1}$	1.4707	1.0718	-1.2919e+05

Table 4.8: The fit percentage, ETFE of $\|Q(d)\Delta_Q(\theta,d)\|_\infty$ and the spectral radius of closed-loop systems for different δ

Considering Figure 4.17 and Figure 4.18, the case $\delta = 0$ allows almost identical response with the input sensitivity function, but it has worse performance on the output trajectory.

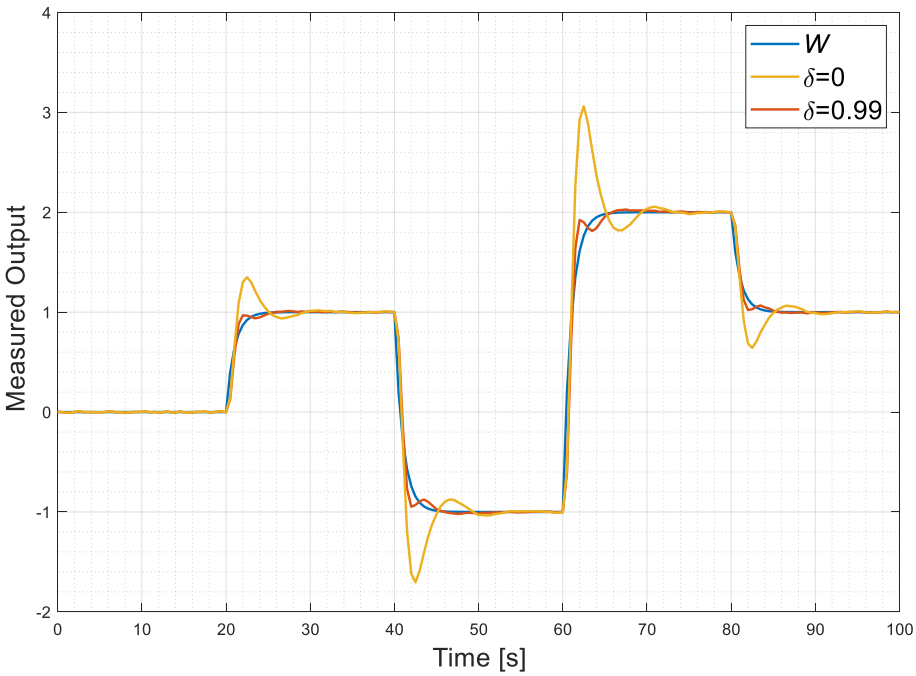

Figure 4.17: Output Trajectories of desired output sensitivity function, $\delta = 0$ and $\delta = 0.99$ cases

On the other hand, $\delta = 0.99$ guarantees closer performance to the desired output sensitivity. Since also this case the stability test is verified for $\tilde{\alpha} = 0.2$, we use it for further comparisons. Note that, however, the case $\delta = 1$ is falsified by the stability test.

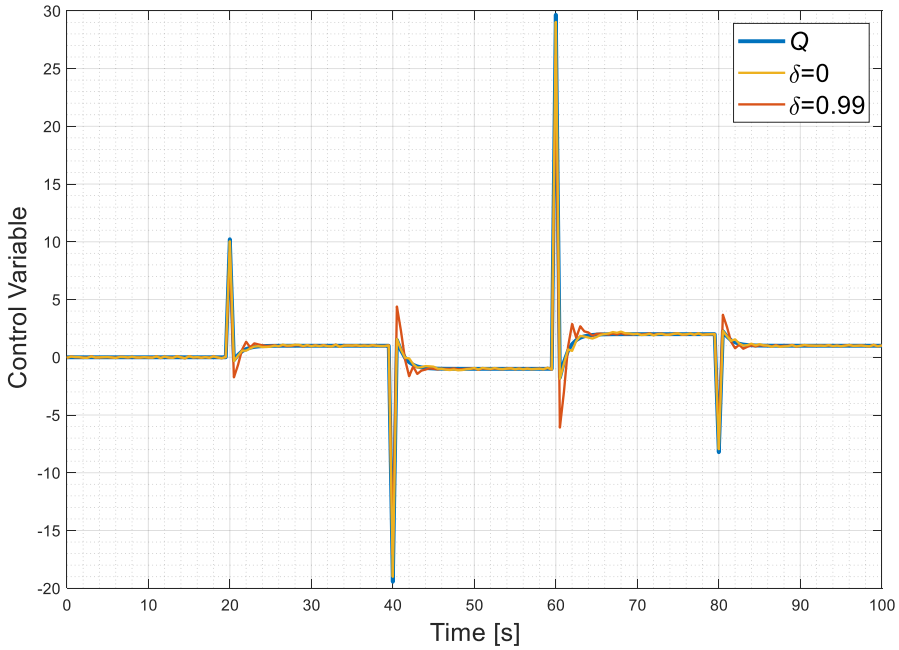

Figure 4.18: Input trajectories of desired input sensitivity function, $\delta = 0$ and $\delta = 0.99$ cases

While implementing the algorithm, each ETFE is smoothed using Hamming Window that yields frequency resolution of about $\pi/200$ and the Bode diagram in case $\delta = 0.99$ for both smoothed and original cases is depicted in Figure 4.19.

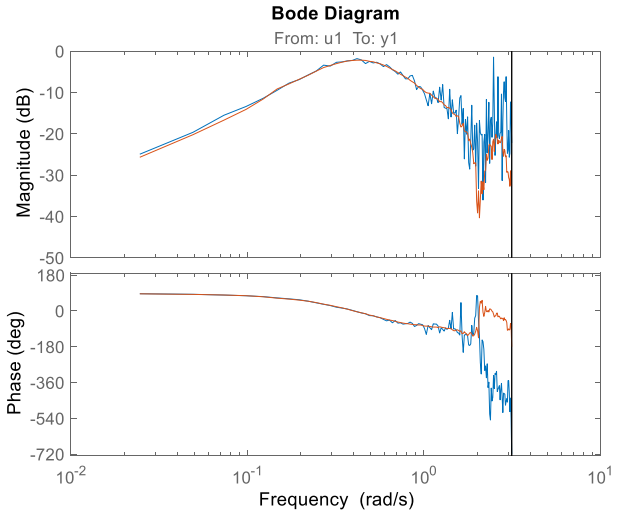

Figure 4.19: Bode diagram of ETFE of $\left\|Q(d)\Delta_Q(\theta,d)\right\|_\infty$ for $\delta = 0.99$ while its smoothed version is in red

4.8.2.2 Comparison with the proposed approach

In this section we show the results obtained with the data-driven methods proposed in Chapter 3 in case of second-order reference models and the results are compared with the results obtained in case $\delta = 0.99$ from previous section.

According to Table 4.9, all approaches allow to achieve good performances. Nevertheless, Case II has the highest $FIT(\%)$. However, the second-order reference model allows the most significant improvement on especially for the unfalsification method results.

		Spectral Radius $\rho(F)$	**Fit Percentage** $FIT(\%)$
Case I		0.8409	92.5904
Case II		0.8417	92.6040
Case III		0.6935	72.3468
	ETFE of $\|\boldsymbol{Q}(\boldsymbol{d})\boldsymbol{\Delta}_{\boldsymbol{Q}}(\boldsymbol{\theta},\boldsymbol{d})\|_{\infty}$	**Spectral Radius** $\rho(F)$	**Fit Percentage** $FIT(\%)$
$\boldsymbol{\delta = 0.99}$	0.7790	0.8079	91.0705

Table 4.9: Performance indexes for validation

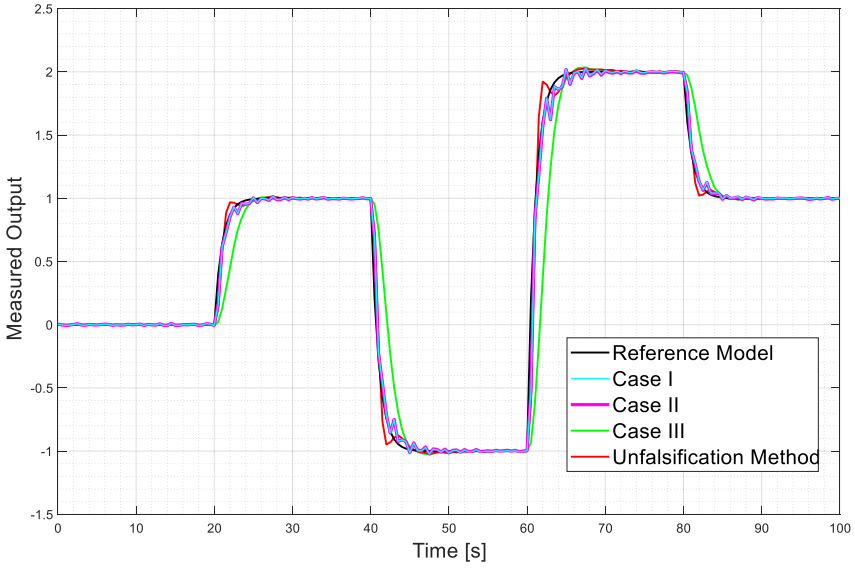

Figure 4.20: Output trajectories of Reference Model, Case I, Case II, Case III and UF with $\delta = 0.99$

According to Figure 4.21, Case III draws attention with the smallest control effort on the system. While Case I, Case II and the unfalsification method require more effective control actions.

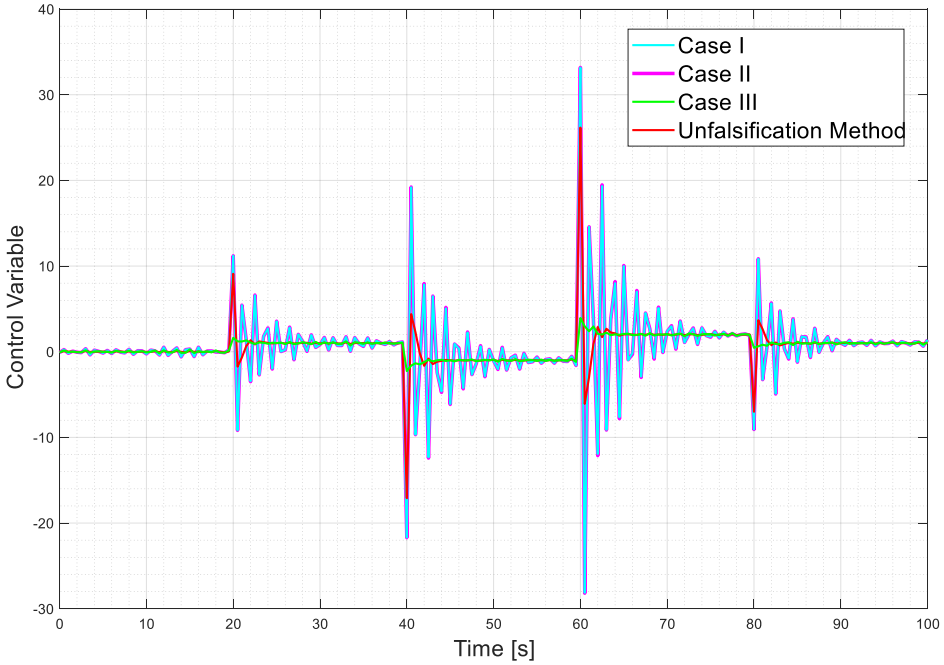

Figure 4.21: Input trajectories of Case I, Case II, Case III and UF with $\delta = 0.99$

4.8.3 Increasing standard deviation of random noise

In this part we compare the discussed data-driven methods when the reference models are first-order, but the data is "more noisy". Remarkably, such change also affects the "Feasible Parameter Set" step of the proposed approach. Therefore, all steps are needed to be redone starting from the dataset collection.

The new batch of data consists of 10000 input-output pairs is collected with an open-loop experiment. The input is again a multilevel pseudo-random signal (MPRS) that uniformly selected between $[-1,1]$ and has switching period of T_s, i.e., 0.5 s for first half of the data and has switching period of $50T_s$, i.e., 25 s for the other half. The output measurement is affected by a measurement noise which varies uniformly at each time step in the range [-0.01,0.01] (The limits of the range are doubled compared to Section 4.8.1). The corresponding signal to noise ratio (SNR) is 37.1691 dB. The input and output measurements are shown in Figure 4.22.

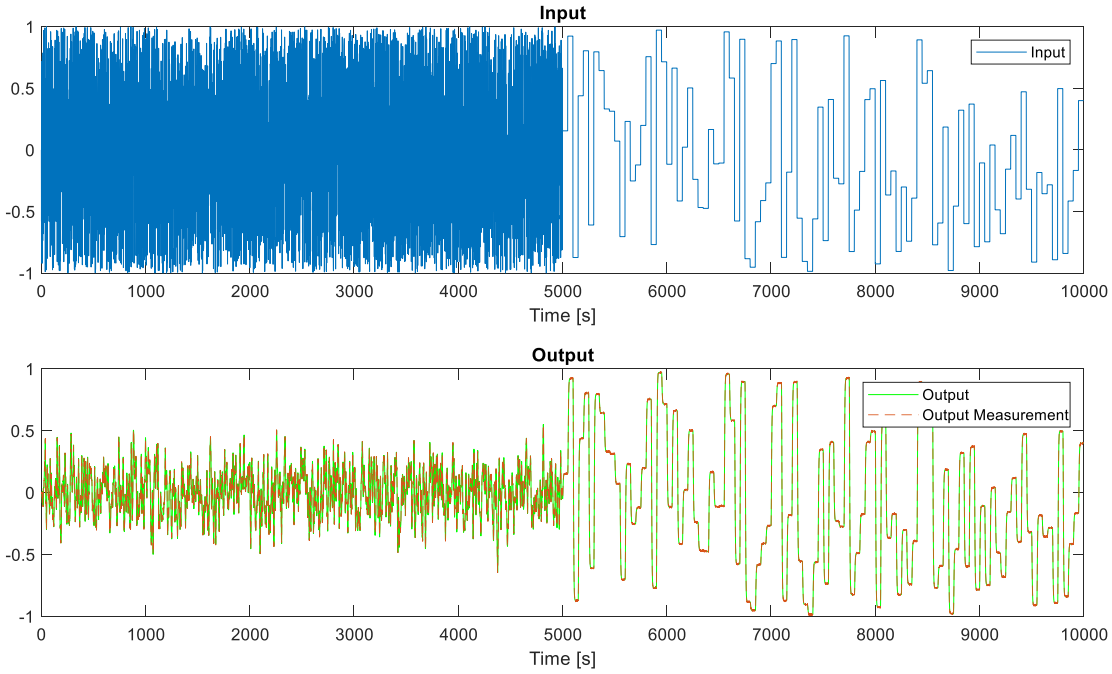

Figure 4.22: Input and output measurements of the open-loop experiment

In order to find the global error bound estimation, equation (2.55) is used with inflation parameter $\alpha = 1.4$ (in Section 4.8.1 it was 1.2). The corresponding feasible parameter set $\widetilde{\Theta}$ consists of 7872 vertices. From Figure 4.23, we can observe that the real parameter set is included in the FPS. Furthermore, the pairs F^i and G^i are also computed for all $i = 1, \dots, 7872$ for future steps.

The desired complementary sensitivity function $W(z)$ and the reference model $M(z)$ and the desired input sensitivity function $Q(z)$ are the same as in Section 4.8.1 and listed below

$$W(z) = M(z) = \frac{0.4z^{-1}}{1 - 0.6z^{-1}} \tag{4.17a}$$

$$Q(z) = \frac{1}{\hat{P}(1)} \frac{(1 - 0.02z^{-1})}{1 - 0.6z^{-1}} \frac{0.4}{0.98} \tag{4.17b}$$

where $\hat{P}(1)$ is the estimated system gain and accepted as 1.

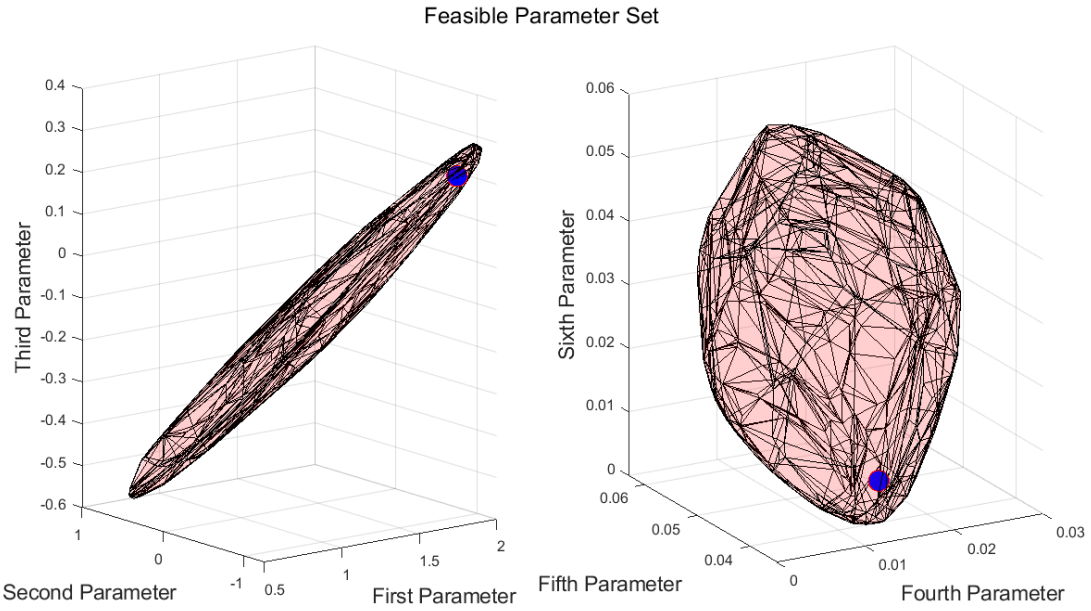

Figure 4.23: Feasible Parameter Set (blue spheres correspond to the real parameters)

4.8.3.1 *Implementation of direct control design based on controller unfalsification with stability guarantees*

In this section we implement the direct control design method discussed in Section 2.2.

According to Figure 4.24 and Table 4.10, the case $\delta = 0$ provides poor performance, although it guarantees closed-loop stability. On the other hand, for increasing values of δ, the output response is closer to the one corresponding with the desired output sensitivity function. If $\tilde{\alpha} = 0.2$ is considered, $\delta = 0.8$ becomes the best solution.

	ETFE of $\|Q(d)\Delta_Q(\theta,d)\|_\infty$	**Spectral Radius $\rho(F)$**	**Fit Percentage $FIT(\%)$**
$\boldsymbol{\delta = 0}$	0.5689	0.8636	57.9273
$\boldsymbol{\delta = 0.75}$	0.9356	0.8146	77.4557
$\boldsymbol{\delta = 0.8}$	0.9535	0.7936	78.5318
$\boldsymbol{\delta = 0.85}$	1.0160	0.8200	80.9402

Table 4.10: The fit percentage, ETFE of $\|Q(d)\Delta_Q(\theta,d)\|_\infty$ and the spectral radius of closed-loop systems for different δ values

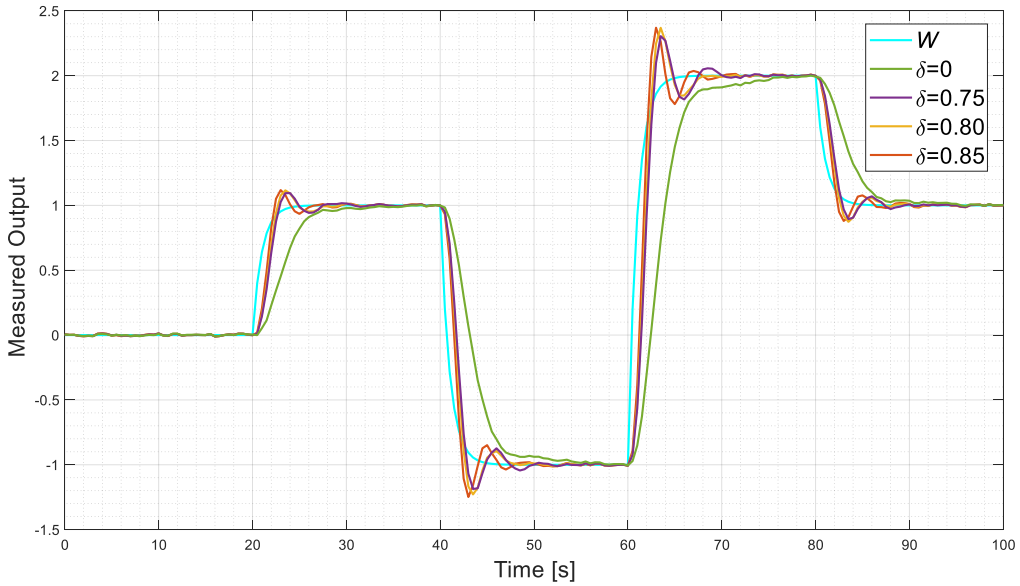

Figure 4.24: Output Trajectories of desired output sensitivity function, $\delta = 0$, $\delta = 0.75$, $\delta = 0.8$ and $\delta = 0.85$ cases

Note that, from Figure 4.25, it can be seen that, for decreasing values of δ, the input is closer and closer with the one provided by the desired input sensitivity function.

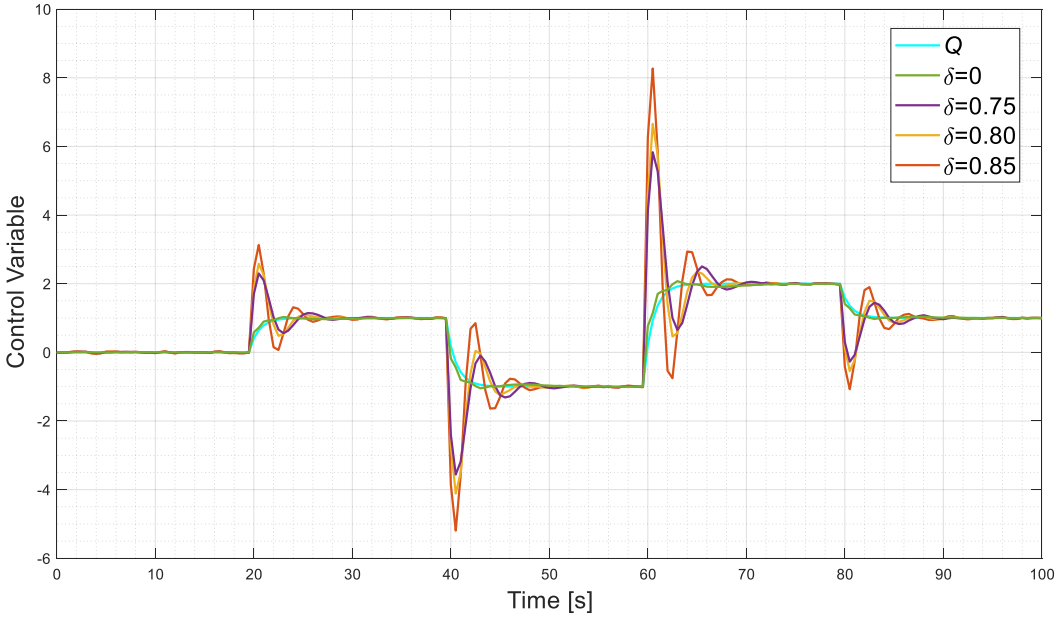

Figure 4.25: Input trajectories of desired input sensitivity function, $\delta = 0$, $\delta = 0.75$, $\delta = 0.8$ and $\delta = 0.85$ cases

While implementing the algorithm, each ETFE is smoothed using Hamming Window that yields frequency resolution of about $\pi/200$ and ETFE of $\left\|Q(d)\Delta_Q(\theta,d)\right\|_\infty$, see Figure 4.26.

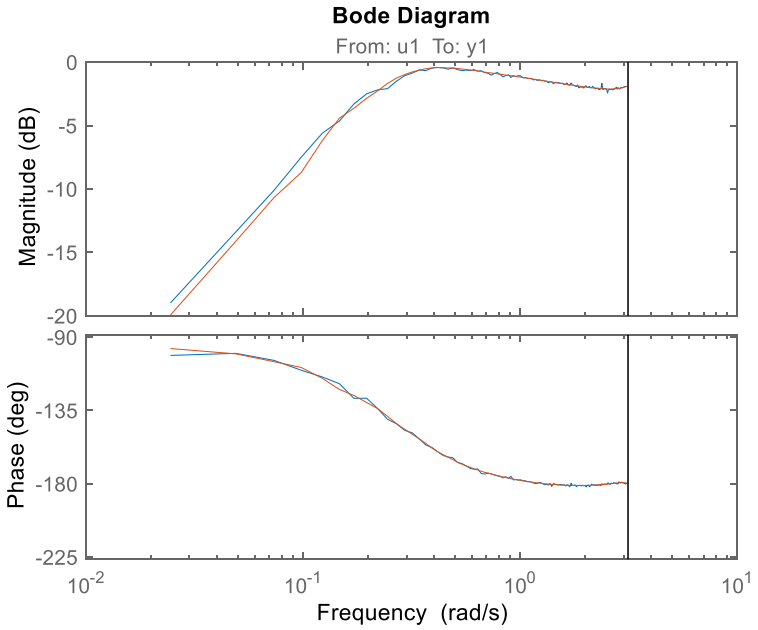

Figure 4.26: Bode diagram of ETFE of $\left\|Q(d)\Delta_Q(\theta,d)\right\|_\infty$ for $\delta = 0.8$ while smoothed version is in red

4.8.3.2 *Comparison with the proposed approach*

In this section the results obtained in case $\delta = 0.8$ are compared with the ones obtained with the data-driven methods proposed in Chapter 3.

From Table 4.11, we can see that all approaches meet the requirements. Indeed, if we compare Table 4.11 with Table 4.7, we can see that Case III and the unfalsification method are less affected by the increase on noise than Case I and Case II. We can interpret that the intrinsic integrator term, that both these methods have, induces the preservation of good performances. On the other hand, the decrease on $FIT(\%)$ can be observed for Case I and Case II.

	Spectral Radius $\rho(F)$	**Fit Percentage** $FIT(\%)$
Case I	0.7602	91.1989
Case II	0.7574	91.1849
Case III	0.8329	81.7079

	ETFE of $\|Q(d)\Delta_Q(\theta,d)\|_\infty$	Spectral Radius $\rho(F)$	Fit Percentage $FIT(\%)$
$\boldsymbol{\delta = 0.8}$	0.9535	0.7936	78.5318

Table 4.11: Performance indexes for validation

Furthermore, according to Figure 4.28 and 4.27, Case I and Case II require more reactive control actions, however, they have better fitting with respect to the reference model.

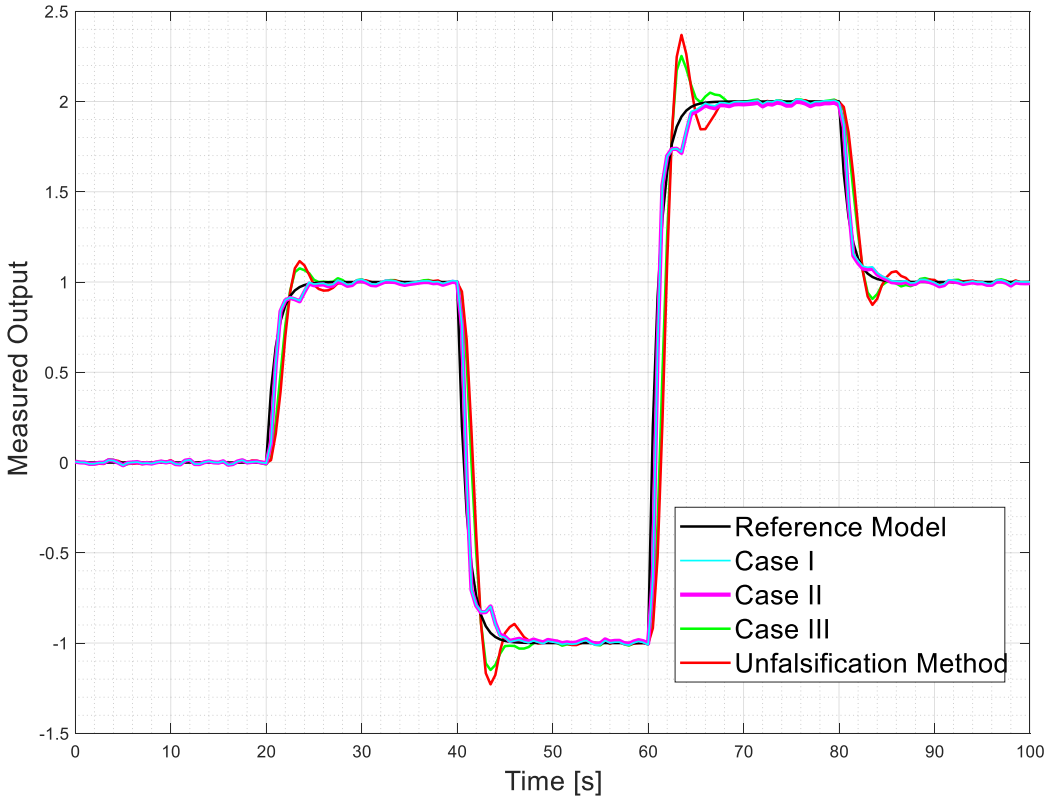

Figure 4.27: Output trajectories of Reference Model, Case I, Case II, Case III and UF with $\delta = 0.8$

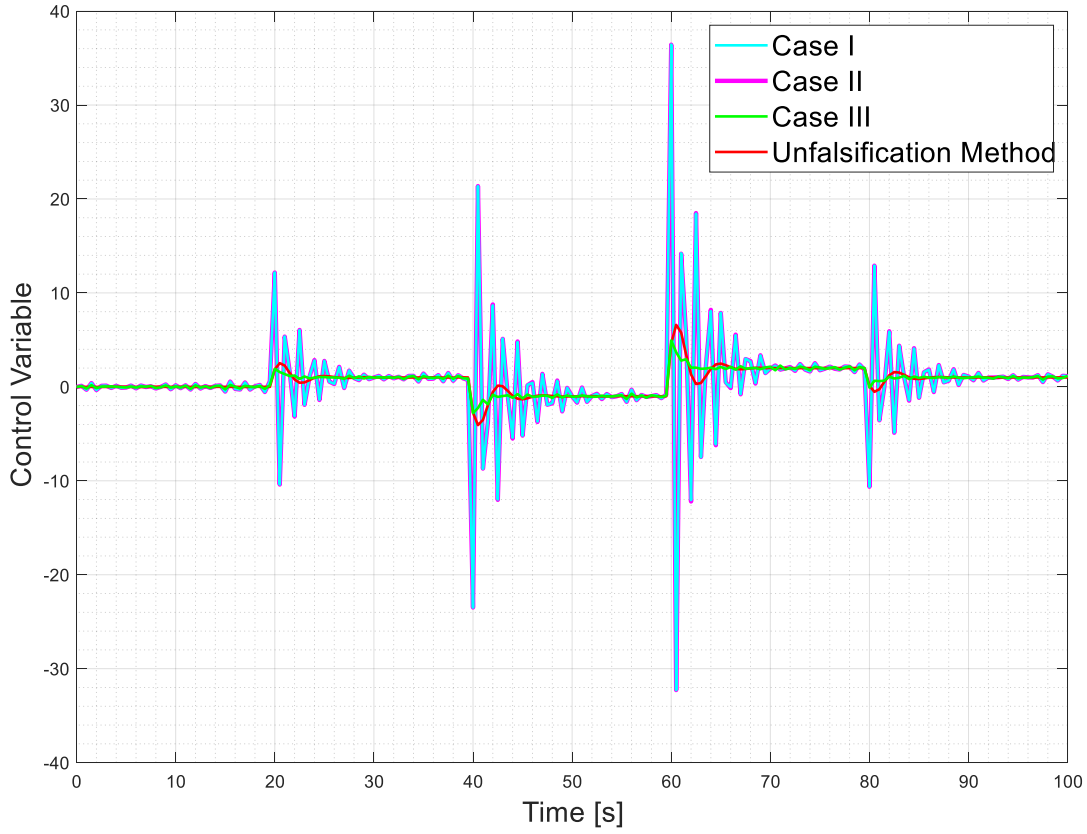

Figure 4.28: Input trajectories of Case I, Case II, Case III and UF with $\delta = 0.8$

5. Conclusion and future development

The purpose of the thesis was to develop a data-based control method for SISO systems with stability guarantees inspired by VRFT and SM. These two methodologies have been combined, allowing to enforce closed-loop stability under suitable conditions during the control design phase.

Firstly, VRFT, direct control design based on controller unfalsification with stability guarantees and SM identification have been recalled from a theoretical point of view.

Secondly, the proposed method has been applied in three cases.

Lastly, the proposed approach has been validated on the simulation of a system with three cascaded tanks. All the simulation results have proven the effectiveness of the proposed approach.

Future extensions will include the extension of the algorithm on more challenging scenarios such as time-varying, nonlinear, or multi-input-multi-output (MIMO) systems. The large control effort in Case I and Case II, and the high frequency components on control variable even in at steady-state in Case III will also be investigated. Also, the reference model optimization could be combined with the proposed approach.

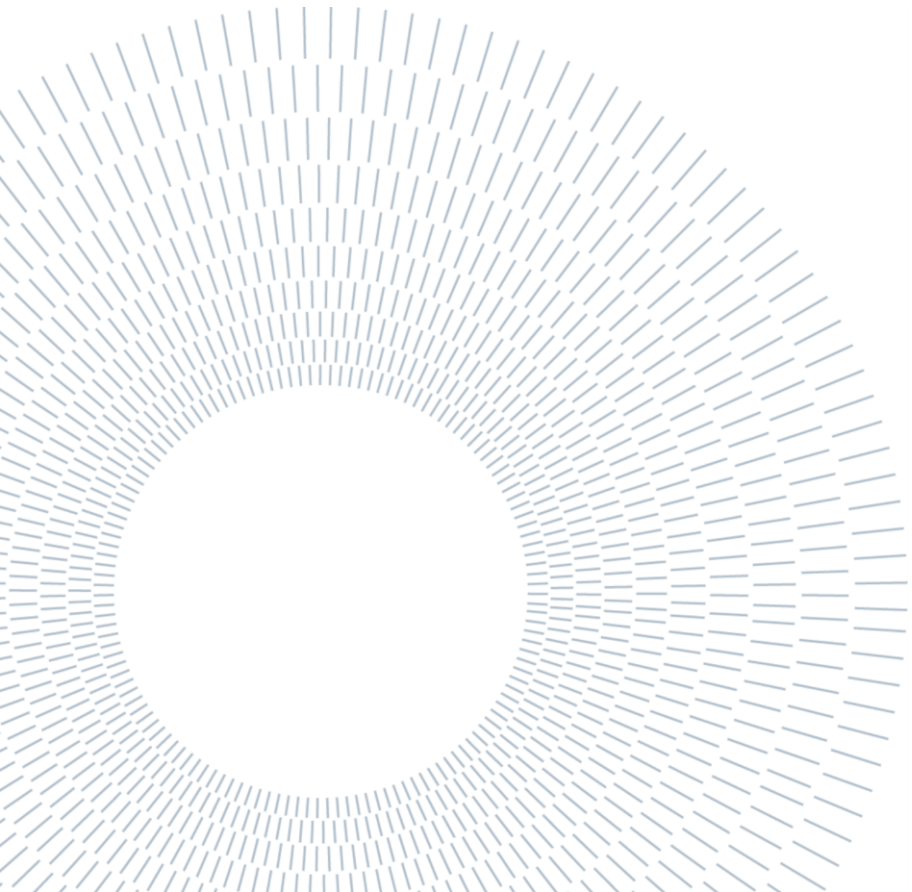

Bibliography

[1] Battistelli, G., Mari, D., Selvi, D., & Tesi, P. (2017). Direct control design via Controller Unfalsification. *International Journal of Robust and Nonlinear Control*, *28*(12), 3694–3712. https://doi.org/10.1002/rnc.3778

[2] Terzi, E., Fagiano, L., Farina, M., & Scattolini, R. (2019). Learning-based predictive control for linear systems: A unitary approach. *Automatica*, *108*, 108473. https://doi.org/10.1016/j.automatica.2019.06.025

[3] Cuzzola, F. A., Geromel, J. C., & Morari, M. (2001). An improved discrete-time robust approach for constrained model predictive control. *2001 European Control Conference (ECC)*. https://doi.org/10.23919/ecc.2001.7076519

[4] Bemporad, A., Garulli, A., Paoletti, S., & Vicino, A. (2003). Set membership identification of piecewise affine models. *IFAC Proceedings Volumes*, *36*(16), 1789–1794. https://doi.org/10.1016/s1474-6670(17)35019-x

[5] Milanese, M., & Novara, C. (2004). Set membership identification of Nonlinear Systems. *Automatica*, *40*(6), 957–975. https://doi.org/10.1016/j.automatica.2004.02.002

[6] Canale, M., Fagiano, L., & Signorile, M. C. (2012). Nonlinear model predictive control from data: A set membership approach. *International Journal of Robust and Nonlinear Control*, *24*(1), 123–139. https://doi.org/10.1002/rnc.2878

[7] Terzi, E., Farina, M., Fagiano, L., & Scattolini, R. (2018). Robust predictive control with data-based multi-step prediction models. *2018 European Control Conference (ECC)*. https://doi.org/10.23919/ecc.2018.8550537

[8] Terzi, E., Fagiano, L., Farina, M., & Scattolini, R. (2018). Learning multi-step prediction models for receding Horizon Control. *2018 European Control Conference (ECC)*. https://doi.org/10.23919/ecc.2018.8550494

[9] Tanaskovic, M., Fagiano, L., & Gligorovski, V. (2019). Adaptive model predictive control for linear time varying MIMO Systems. *Automatica*, *105*, 237–245. https://doi.org/10.1016/j.automatica.2019.03.030

[10] Milanese, M., & Novara, C. (2005). Model quality in identification of Nonlinear Systems. *IEEE Transactions on Automatic Control*, *50*(10), 1606–1611. https://doi.org/10.1109/tac.2005.856657

[11] Milanese, M., & Novara, C. (2009). Set membership methods in identification, prediction and filtering of Nonlinear Systems. *IFAC Proceedings Volumes*, *42*(10), 263–272. https://doi.org/10.3182/20090706-3-fr-2004.00044

[12] Lauricella, M., & Fagiano, L. (2020). Set membership identification of linear systems with guaranteed simulation accuracy. *IEEE Transactions on Automatic Control*, *65*(12), 5189–5204. https://doi.org/10.1109/tac.2020.2970146

[13] Milanese, M., Norton, J., Piet-Lahanier, H., & Walter, E. (1996). Bounding approaches to system identification. New York: Plenum Press.

[14] Betti, G., Farina, M., & Scattolini, R. (2013). A robust MPC algorithm for offset-free tracking of constant reference signals. *IEEE Transactions on Automatic Control*, *58*(9), 2394–2400. https://doi.org/10.1109/tac.2013.2254011

[15] Ozay, N., Lagoa, C., & Sznaier, M. (2015). Set membership identification of switched linear systems with known number of subsystems. *Automatica*, *51*, 180–191. https://doi.org/10.1016/j.automatica.2014.10.101

[16] Wang, H., Kolmanovsky, I. V., & Sun, J. (2018). Zonotope-based recursive estimation of the feasible solution set for linear static systems with additive and multiplicative uncertainties. *Automatica*, *95*, 236–245. https://doi.org/10.1016/j.automatica.2018.05.035

[17] Campi, M. C., & Savaresi, S. M. (2006). Direct nonlinear control design: The virtual reference feedback tuning (VRFT) approach. *IEEE Transactions on Automatic Control*, *51*(1), 14–27. https://doi.org/10.1109/tac.2005.861689

[18] W. D'Amico, M. Farina, G. Panzani, Advanced control based on recurrent neural networks learned using virtual reference feedback tuning and application to an electronic throttle body (with supplementary material), arXiv preprint arXiv:2103.02567.

[19] H. Ichihara and A. Kiyotani, "Virtual reference feedback tuning for MIMO plants by subspace identification," 2015 European Control Conference (ECC), 2015, pp. 830-835, doi: 10.1109/ECC.2015.7330645.

[20] Lecchini, A., Campi, M. C., & Savaresi, S. M. (2002). Virtual reference feedback tuning for two degree of Freedom Controllers. *International Journal of Adaptive Control and Signal Processing*, *16*(5), 355–371. https://doi.org/10.1002/acs.711

[21] Campi, M. C., Lecchini, A., & Savaresi, S. M. (2002). Virtual reference feedback tuning: A direct method for the design of feedback controllers. *Automatica*, *38*(8), 1337–1346. https://doi.org/10.1016/s0005-1098(02)00032-8

[22] Gonçalves da Silva, G. R., Bazanella, A. S., & Campestrini, L. (2020). One-shot data-driven Controller Certification. *ISA Transactions*, *99*, 361–373. https://doi.org/10.1016/j.isatra.2019.10.011

[23] Vinnicombe, G. (1993). Frequency domain uncertainty and the graph topology. *IEEE Transactions on Automatic Control*, *38*(9), 1371–1383. https://doi.org/10.1109/9.237648

[24] M. G. Safonov and Tung-Ching Tsao, "The unfalsified control concept and learning," in IEEE Transactions on Automatic Control, vol. 42, no. 6, pp. 843-847, June 1997, doi: 10.1109/9.587340.

[25] Selvi, D., Piga, D., Battistelli, G., & Bemporad, A. (2021). Optimal direct data-driven control with stability guarantees. *European Journal of Control*, *59*, 175–187. https://doi.org/10.1016/j.ejcon.2020.09.005

[26] A. Karimi, K. van Heusden and D. Bonvin, "Non-iterative data-driven controller tuning using the correlation approach," 2007 European Control Conference (ECC), 2007, pp. 5189-5195, doi: 10.23919/ECC.2007.7068802.

[27] Hjalmarsson, H. (1998). Iterative feedback tuning. *IFAC Proceedings Volumes*, *31*(22), 101–108. https://doi.org/10.1016/s1474-6670(17)35928-1

[28] Luo, X.-S., & Song, Y.-D. (2018). Data-driven predictive control of Hammerstein–Wiener Systems based on subspace identification. *Information Sciences*, *422*, 447–461. https://doi.org/10.1016/j.ins.2017.09.004

[29] Bobal, V., Kubalcik, M., Dostal, P., & Matejicek, J. (2013). Adaptive predictive control of time-delay systems. *Computers & Mathematics with Applications*, *66*(2), 165–176. https://doi.org/10.1016/j.camwa.2013.01.035

[30] Terzi, Enrico & Farina, Marcello & Scattolini, Riccardo. (2019). Model predictive control design for dynamical systems learned by Long Short-Term Memory Networks.

[31] Safonov, Michael & Cheong, Shin-Young. (2006). Unfalsified Control: Theory and Applications

[32] Matt J (2022). *Analyze N-dimensional Convex Polyhedra* (https://www.mathworks.com/matlabcentral/fileexchange/30892-analyze-n-dimensional-convex-polyhedra), MATLAB Central File Exchange. Retrieved March 6, 2022.

[33] Lofberg, J. (n.d.). Yalmip: A toolbox for modeling and optimization in MATLAB. *2004 IEEE International Conference on Robotics and Automation (IEEE Cat. No.04CH37508)*. https://doi.org/10.1109/cacsd.2004.1393890

[34] *Mosek modeling Cookbook*. MOSEK Modeling Cookbook - MOSEK Modeling Cookbook 3.2.3. (n.d.). Retrieved March 20, 2022, from https://docs.mosek.com/modeling-cookbook/index.html#

List of Figures

List of Tables

Acknowledgements

I would first like to express my sincere gratitude to my advisor, Prof. Marcello Farina. He has guided me with his immense knowledge from the initial step in work enabled me to develop an understanding of the subject. He encouraged me to carry on with all his patience and support. It is an honor to learn from Prof. Farina.

I wish to extend my sincere gratitude to my co-advisor, Ing. William D'Amico. He has always been there with his continuous support, invaluable supervision, and patience to help me whenever I had a question about my research or writing.

I am also grateful to my family members: my mother Sevim, my father Bünyamin, my brother Anıl and his wife Yağmur; without their deep understanding and support, it would be impossible for me to complete the thesis.

Finally, I would like to thank my girlfriend, Simge, for her unwavering support and belief in me.